[AMERICAN JOURNAL OF SCIENCE, VOL. 321, JANUARY-FEBRUARY, 2021, P. 152–177, DOI 10.2475/01.2021.04]

SHRIMP U-Pb DATING OF DETRITAL ZIRCONS FROM THE PERMIAN SANDSTONES ALONG THE SOUTHERN AND NORTHERN MARGINS OF XAR MORON RIVER, CENTRAL INNER MOGOLIA: IMPLICATIONS FOR PROVENANCE AND THE TECTONIC EVOLUTION OF THE EASTERN SEGMENT OF THE CENTRAL ASIAN OROGENIC BELT

XIANCAN WU*, YURUO SHI*,†, and J. LAWFORD ANDERSON**

ABSTRACT. The Xar Moron River fault zone, located in the eastern segment of the Central Asian Orogenic Belt (CAOB), represents the intensely debated final collision zone of the Siberian Craton (SC) and North China Craton (NCC). To determine the tectonic evolution of the eastern segment of the CAOB, we undertook petrography and zircon U-Pb dating of the Huanggangliang and Linxi formations in the Wufendi and Xingfuzhilu areas along the Xar Moron River. Petrographic analysis of Permian sandstones revealed a close relationship between the sedimentary and orogenic sources suggesting short transport distances. A sample from the Huanggangliang Formation yielded detrital zircon U-Pb ages ranging from 2653 Ma to 265 Ma, with three age populations: at 2653 to 2443 Ma, 1935 to 1764 Ma, and 482 to 265 Ma, whereas samples from the Linxi Formation yielded detrital zircon U-Pb ages ranging from 3363 Ma to 257 Ma, with four age populations: at 2705 to 2403 Ma, 2011 to 1203 Ma, 571 to 375 Ma, and 356 to 257 Ma. The age spectrum differences of sandstones on both banks indicate that the Xar Moron River fault zone is the final collision zone of the eastern segment of the CAOB. The sandstone of Huanggangliang Formation yielded a weighted mean age of 265.7 ± 1.5 Ma, suggesting that the main deposition of the Huanggangliang Formation was during the Middle Permian. In addition, a comparison of the youngest age in the sedimentary rocks with U-Pb ages obtained for pyroclastic rock implies that the Linxi Formation formed in the late Permian. The results of our study support the view that the final closure of the eastern segment of Paleo-Asian Ocean (PAO) occurred during late Permian to earliest Triassic times.

Key words: Xar Moron River, Central Asian Orogenic Belt, Huanggangliang and Linxi Formations, detrital zircon U-Pb isotopic dating, Paleo-Asian Ocean

INTRODUCTION

The Central Asian Orogenic Belt (CAOB), also known as the Altaids (Sengör and others, 1993; Sengör and Natal'in, 1996), is the largest accretionary orogen in the world (Sengör and Natal'in, 1996), which formed by accretion of island arcs, ophiolites, oceanic islands, seamounts, accretionary wedges, oceanic plateaus and microcontinents and evolved from about 1000 Ma to 250 Ma (Jahn and others, 2000; Kröner and others, 2007; Windley and others, 2007; Han and others, 2015; Zhang and others, 2016; Liu and others, 2017a). This enormous orogenic belt extends from the Urals via Kazakhstan, Tien Shan, Altai, and Mongolia to the Pacific (Windley and others, 2007; Jian and others, 2008; Liu and others, 2017a; Zhou and others, 2018) and lies between the Siberian Craton (SC) to the north, the Tarim and North China (NCC) cratons to the south and the East European Craton to the west (Jian and others, 2008; Xiao and others, 2013; Xiao and others, 2015, fig. 1A). The CAOB underwent a complicated process of arc-continent collision that recorded the breakup of the Rodinia supercontinent and the creation of the Eurasian supercontinent (Xiao

* Beijing SHRIMP Center, Institute of Geology, Chinese Academy of Geological Sciences, Beijing 100037, China
** Department of Earth and Environment, Boston University, Boston, Massachusetts 02215, USA
† Corresponding author: 26 Baiwanzhuang Road, Beijing 100037, China. Tel.: +86 10 68999766 shiyuruo@bjshrimp.cn

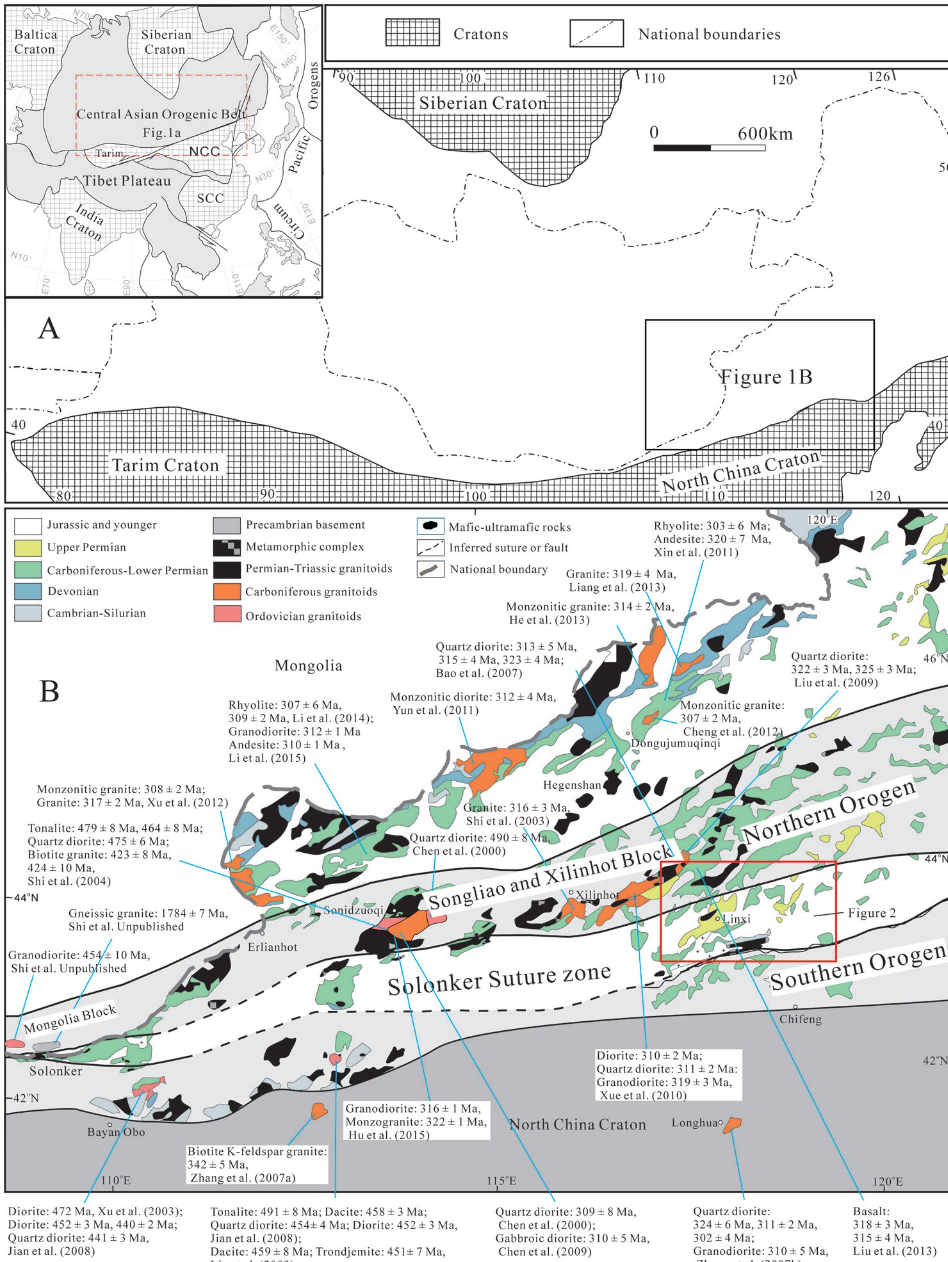

Fig. 1. (A) Outline map of the southeastern CAOB (modified after Jahn and others, 2000; Jian and others, 2010; Shi and others, 2018; the inset map of figure 1A compiled after Jahn and others, 2000). (B) Sketch geological map of the eastern segment of the CAOB (modified after Jian and others, 2010; Shi and others, 2016).

and others, 2003; Windley and others, 2007; Li and others, 2008; Kröner and others, 2015; Zhao and others, 2018). Despite numerous investigations, there are still many controversies mainly related to the timing and suture zone locations of the block amalgamations and the final closure time of the Paleo-Asian Ocean (PAO, Sengör and others, 1993; Liu and others, 2017a; Eizenhöfer and Zhao, 2018, and references therein). At present, most scholars agree that the Solonker Suture Zone (SSZ) was the last collision suture zone of the North China and the Siberian cratons (Sengör and Natal'in, 1996; Li, 2006; Windley and others, 2007; Xiao and others, 2015; Xiao and others, 2018). According to the regional structure and stratigraphic characteristics, it has been proposed that the two plates collided during the Late Devonian to Early Carboniferous (Tang, 1990; Shao, 1991; Xu and Chen, 1997), at the Late Permian (Sengör and Natal'in, 1996), or during the Late Permian and Middle Triassic (Xiao and others, 2003, 2015; Li, 2006; Li and others, 2009; Zhang and others, 2009; Eizenhöfer and others, 2014).

The Xing'an-Mongolian Orogenic Belt (XMOB) (fig. 1B) comprises the main part of the eastern segment of the CAOB, with the Siberian Craton in the north, the North China Craton in the south, and the western Pacific Plate in the east (Sengör and Natal'in, 1996; Jahn and others, 2004; Li and others, 2006). It records a huge amount of information regarding how the two blocks (NCC and SC) amalgamated and the subsequent subduction of the West Pacific plate underneath the Eurasian continent. It is vital not only for understanding the sedimentary formation of the CAOB but also to recognizing its interaction with surrounding tectonic units (Windley and others, 2007; Li and others, 2013). There are two different views on the tectonic evolution of this region since the early Paleozoic, especially on the final closure time and location of the PAO in recent years.

Some workers have suggested that the final suture of the CAOB was along the Hegenshan ophiolite belt or even further north along the mélange zone of South Mongolia (Tang, 1990; Bao and others, 2007; Liu and others, 2009). However, a popular interpretation about the tectonic history of the CAOB is that the SSZ marked the final amalgamation of this area (Li and others, 2006; Li and others, 2009; Zhang and others, 2009; Xiao and others, 2009; Eizenhöfer and others, 2014; Xiao and others, 2015). The main two views on the final closure time of the PAO are as follows: (1) the collision occurred in the late Permian to Early Triassic (Eizenhöfer and Zhao, 2018; Xiao and others, 2018; Wu and others, 2020) and that the evolution of the XMOB was similar to that of the Pacific Rim accretionary orogen. During the Paleozoic, there were multi-period subduction and island arc accretion processes in the PAO (Chen and others, 2000; Miao and others, 2008; Song and others, 2015), which formed the Hegenshan and Baolidao subduction-accretion systems in the north, and the Ondor Sum subduction-accretion system in the south (Xiao and others, 2003); (2) the collision occurred in the late Silurian or Early-Middle Devonian (Tang, 1990; Shao, 1991; Xu and others, 2013) and that the Central Inner Mongolia region entered a new crustal evolution stage under an extensional tectonic setting from the Carboniferous to Permian (Shao and others, 2014).

Even so, compared with the well-researched NW China region of the western CAOB (Xiao and others, 2003; Windley and others, 2007; Kröner and others, 2010; Pirajno and others, 2011; Tang and others, 2015; Xiao and others, 2015; Liu and others, 2017c, 2017d; Han and Zhao, 2018), current research is relatively weak in the eastern segment of the CAOB. Our current work is to better understand the interaction between respective tectonic elements within the PAO and the provenance contribution and relation of surrounding blocks to involved sedimentary basins. One of the effective methods to resolve the above disputes is to make a detailed study of the sedimentary formations at the end of late Palaeozoic in key areas.

The Solonker-Xar Moron Suture Zone has long been considered to mark the location of the final disappearance of the PAO in the eastern segment of the CAOB (Xiao and others, 2003; Liu and others, 2017a), which is one of the most significant suture zones formed during the evolution of the eastern segment of the CAOB. The Huanggangliang and Linxi formations in central Inner Mongolia occur on both sides of the Xar Moron River, respectively, which provide information on relationships between major tectonic blocks. Major tectonic units can be identified by comparing age distributions of sandstones from two sides of the Xar Moron River to well-defined "age-fingerprints" of likely provenance terrane candidates (Eizenhöfer and others, 2014). Detrital zircons in sandstone are resistant to weathering and possess an inherently stable U-Pb isotopic system, which preserve the age record of their original host rocks (Lee and others, 1997; Cherniak and Watson, 2001; Kosler and Sylvester, 2003). Therefore, detrital zircon chronology is a potentially powerful tool to constrain depositional age, sedimentary provenance, regional palaeogeography, and tectonic relationships between major tectonic blocks (Krogh and Keppie, 1990; Lee and others, 1997; Sircombe and Freeman, 1999; Cawood and Nemchin, 1999; Hu and others, 2013). In this present study, an integrated approach incorporating field observation and measurement, framework petrography and detrital zircon U-Pb geochronology has been used to constrain both the provenance and maximum age of deposition of the Huanggangliang and Linxi formations. Our results provide constraints on their position relative to the collision between the North China and Siberian cratons, the final closure time of the PAO, and evidence for the evolution of the tectonic setting of the eastern segment of the CAOB.

GEOLOGICAL SETTING

The SSZ has long been considered to mark the location of the final disappearance of the PAO in the eastern segment of the CAOB (Xiao and others, 2003; Jian and others, 2008) (fig. 1B). This suture zone records the terminal evolution of the CAOB in Inner Mongolia (Xiao and others, 2003) and tectonically separates the two orogenic belts (Sengör and others, 1993), described here as the Southern Orogenic Belt (SOB) and Northern Orogenic Belt (NOB; Jian and others, 2008). A major tectonic unit of the SOB (fig. 1B) includes the Ondor Sum subduction-accretion complex (Hu and others, 1990; Xiao and others, 2003) which contains turbidites, olistostrome mélanges, and blueschists, in a nearly E-W trending ophiolite belt about 200 km long and 25 km wide (Hu and others, 1990; Wang and others, 1991). It also includes the Bainaimiao arc that borders the NCC fault (Hu and others, 1990; Johnson and others, 2001). The NOB (fig. 1B) forms a north-dipping thrust belt, which from south to north includes the Xilinhot metamorphic complex (Tang, 1990), the Erdaojing subduction-accretion complex (Xu and Chen, 1997), and an extensive TTG pluton (Chen and others, 2000; Jian and others, 2008).

The late Paleozoic stratigraphy of the region is discontinuously exposed along the Xar Moron River, whereas upper Paleozoic, especially Permian, strata are more widespread (BGMRIM, 1991, fig. 2). The lithology across the Xar Moron River is dominated by the Linxi and Huanggangliang formations, and some late Paleozoic granitic and undeformed Mesozoic granitic intrusions (fig. 2).

The middle Permian Huanggangliang Formation conformably overlies the Dashizhai Formation and is divided into an upper and a lower member, all of which are dominated by clastic sedimentary rocks. The lower member is 1568 m thick and composed of grayish-green fine-grained sandstone, black slate and sandy conglomerate; the upper member is 1110 m thick and composed of purplish-red sandstone, siltstone, and slate interbedded with conglomerate (BGMRIM, 1991, fig. 3A). The Huanggangliang Formation is a marine sedimentary succession and is unconformably overlain by the generally fine- grained clastic Linxi Formation (BGMRIM, 1991).

The Linxi Formation occupies an extensive area in eastern Inner Mongolia and unconformably overlies the Zhesi Formation (equivalent Permian strata to the south

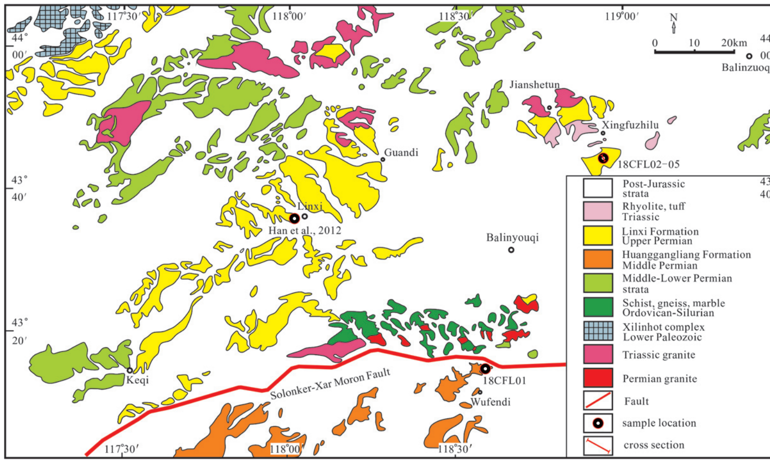

Fig. 2. Sketch geological map of the Xar Moron River region (modified after BGMRIM, 1991; the location is shown in fig. 1B). Sample sites are also given.

of the Xar Moron River are named the Huanggangliang Formation, Shen and others, 2006). It is characterized by alternating sandstone, siltstone, and slate suggesting a turbiditic origin, although typical turbiditic patterns are rare (BGMRIM, 1991, figs. 3B and 3C). In addition, large numbers of bryozoan and sponge spicule fossils were discovered in the thick limestone layers and lenses of the upper part of the Linxi Formation in eastern Inner Mongolia which revealed that the late upper Permian in the Linxi area is consistent with either a marine environment or a marine-dominated sedimentary environment (Zhang and others, 2014a).

SAMPLING AND ANALYTICAL METHODS

We collected sandstone samples from the Huanggangliang and Linxi formation (fig. 2). Our samples of Huanggangliang Formation in the Wufendi area are composed of purplish-red sandstone (fig. 2). Three samples from Linxi Formation were collected from the typical section in the Xingfuzhilu area, where grayish-green fine sandstone, gritstone and conglomerate are exposed. Moreover, one sample was from a tuffaceous pyroclastic rock (figs. 4E and 4F). The sandstone samples were chosen for analysis by SHRIMP U-Pb dating of detrital zircons. The locations of the samples are given in table 1 and are shown in figure 3C.

Samples were first crushed mechanically, sieved and then separated by standard heavy liquid and electromagnetic techniques. Zircons were extracted randomly from the heavy mineral concentrate by hand-picking under a binocular microscope, mounted in epoxy, and polished to expose the cores of individual grains, in order to reveal internal structures. The grain mount was then photographed in reflected light, cleaned, and gold-coated. For SHRIMP U-Pb analysis, grain growth structures were imaged using cathodoluminescence (CL). Cathodoluminescence imaging was done on a scanning electron microscope (HITACHI S3000-N) fitted with a GATAN Chroma at the Beijing SHRIMP Center, Institute of Geology, Chinese Academy of Geological Sciences.

U-Pb zircon ages were obtained using a SHRIMP housed at the Beijing SHRIMP Center, Institute of Geology, Chinese Academy of Geological Sciences, and the analytical procedures followed that of Williams (1997). Spot sizes were 25 to 30 μm and the surface of the analysis site was rastered for 3 min prior to each analysis to remove

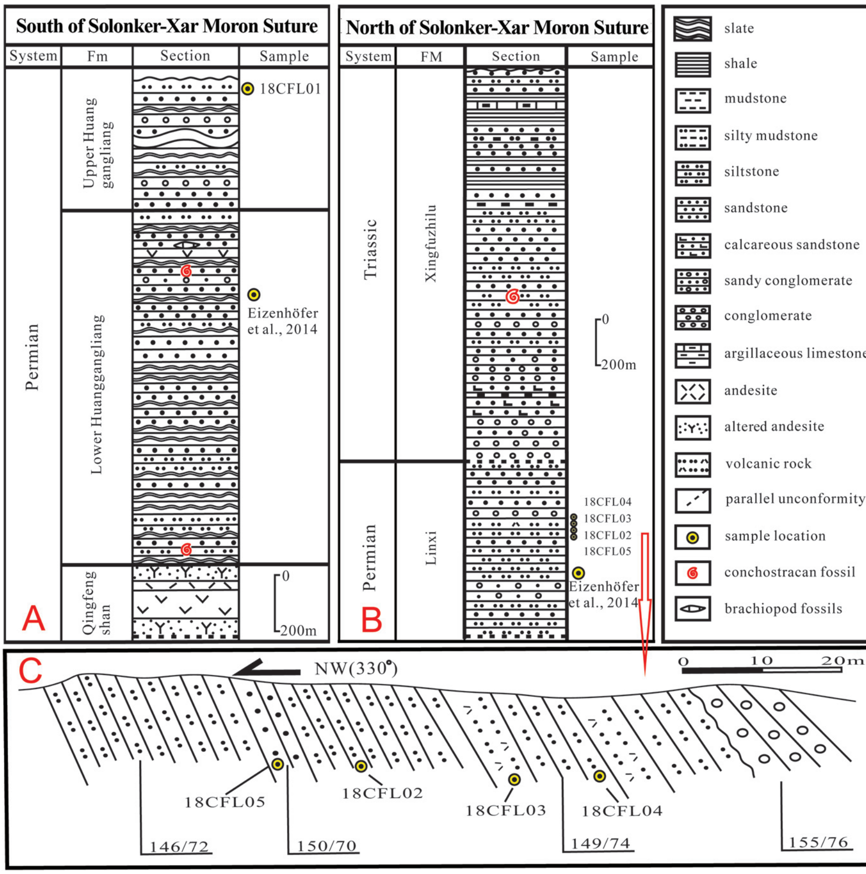

Fig. 3. (A) Permian stratigraphic column of the Wufendi area in the southern of Xar Moron River, (B) stratigraphic column of Triassic-Permian strata of the Xingfuzhilu area in the northern of Xar Moron River (modified after BGMRIM, 1991), (C) a cross section of detailed sequences with structural attitudes from figure 3B.

the gold coating. Data were determined by taking 3 to 5 scans on $^{90}Zr_2{}^{16}O^+$, $^{204}Pb^+$, Background, $^{206}Pb^+$, $^{207}Pb^+$, $^{208}Pb^+$, $^{238}U^+$, $^{232}Th^{16}O^+$, $^{238}U^{16}O^+$. Standard zircon M257, with an age of 561.3 ± 0.3 Ma and U content of 840 ppm (Nasdala and others, 2008), was used to calibrate U and Th content. Reference zircon TEMORA (417 Ma, Black and others, 2003) was analyzed during the session to calibrate the U-Pb age of the unknown. Common Pb corrections were made using the measured ^{204}Pb. Uncertainties for each analysis are at 1σ. Data were processed using the Excel-based Squid (Ludwig, 2001) and Isoplot (Ludwig, 2003) programs.

RESULTS

Sandstone Petrography

The grain size of sample 18CFLO1 of the Huanggangliang Formation (figs. 4A and 4B) is between 1.5 to 2.5 mm, containing moderate quartz (56 wt.%, including 39 wt.% of monocrystalline quartz and 17 wt.% of polycrystalline quartz), and abundant lithic fragments (34 wt.%, mainly igneous fragments), with minor feldspar (2 wt. %, mainly plagioclase) and a minor proportion of muscovite (7 wt.%). The matrix consists of fine-grained lithic fragments, with subordinate white mica and zircon as

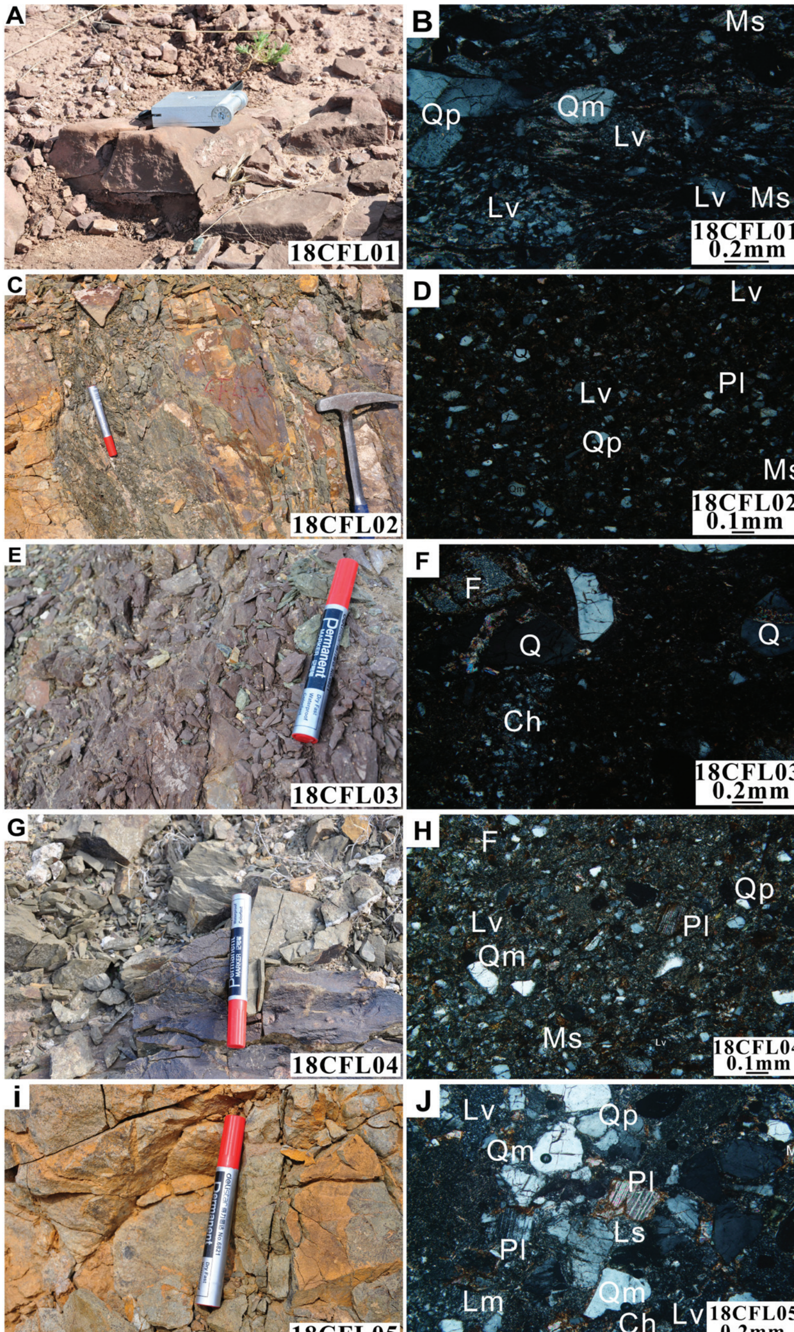

Fig. 4. Field photographs of the studied sandstones (A, C, E, G, I) and photomicrographs of detrital components of (B, D, F, H, J) under cross-polarized light. Abbreviations: Qm, monocrystalline quartz; Pl, plagioclase; Ms, muscovite; Lv, volcanic rock fragment; Lm, metamorphic rock fragment; Ls, sedimentary rock fragment.

TABLE 1

Sandstone Description and GPS Location of the Samples From the Huanggangliang and Linxi formations in the Xar Moron River Region

Sample	GPS	Lithology	grains	Qm(%)	Qp (%)	F (%)	L(%)	Ms(%)	Qt(%)	Lt(%)
				Linxi Formation						
18CFL02	N43°42′05″ E118°57′01″	fine grained lithic graywacke	350	103 (29.43%)	23 (6.57%)	22 (6.29%)	157 (44.86%)	45 (12.86%)	126 (36.00%)	180 (51.43%)
18CFL03	N43°42′04″ E118°57′02″	tuffaceous pyroclastic rock								
18CFL04	N43°42′04″ E118°57′03″	medium grained lithic graywacke	350	114 (32.57%)	17 (4.86%)	13 (3.71%)	165 (47.14%)	41 (11.71%)	131 (37.43%)	182 (52.00%)
18CFL05	N43°42′05″ E118°57′00″	medium grained lithic sandstone	350	122(34.86%)	30(8.57%)	21(6.00%)	154(44.00%)	23(6.57%)	152(43.43%)	184(52.57%)
				Huanggangliang Formation						
18CFL01	N43°14′35″ E118°34′56″	medium grained lithic sandstone	350	136 (38.86%)	60 (17.14%)	8 (2.29%)	120 (34.29%)	26 (7.43%)	196 (56.00%)	180 (51.43%)

Abbreviations: Qm, monocrystalline quartz; Qp, polycrystalline quartz; Qt, total quartz; F, total feldspars; L, lithic fragments; Ms, muscovite; Qt = Qm + Qp; and Lt = L + Qp (polycrystalline quartz).

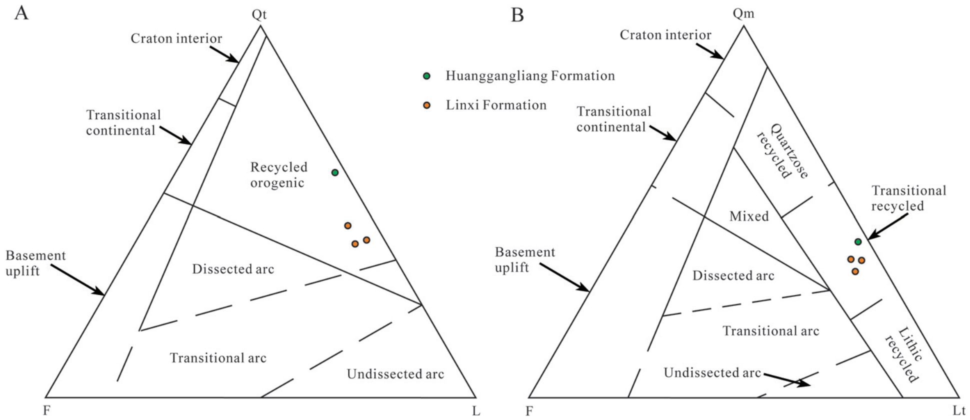

Fig. 5. Discrimination plots of Qt–F–L (A) and Qm–F–Lt (B) (Parameters follow Dickinson and Suczek, 1979; Dickinson and others, 1983; Dickinson, 1985). Abbreviations: Qt, total quartz; Qm, monocrystalline quartz; F, total feldspar; L, lithic fragments; and Lt = L + Qp (polycrystalline quartz).

accessory minerals. The sandstone is immature, with low degrees of rounding and sorting, which indicates short transport and rapid burial (fig. 4B). Moreover, the directional arrangement of quartz and muscovite suggests that they may have undergone deformation. On the plot of Qt–F–L (fig. 5A) and Qm–F–Lt (fig. 5B), the samples fall into the field of recycled orogenic and transitional recycled orogenic, respectively.

The sedimentary rocks of Linxi Formation (figs. 4C, 4D, 4G and 4H) are characterized by a moderate proportion of quartz (36–43 wt.%), minor feldspar (4–6 wt.%), abundant lithic fragments (44–47 wt.%, mainly igneous fragments) and a small proportion of muscovite (7–13 wt.%), except for sample 18CFL05 (figs. 4I and 4J), which is a medium-grained lithic sandstone. Overall the matrix of sandstones from the Linxi Formation mostly consists of fine-grained lithic fragments, with medium to fine-grained texture (1.0–2.5 mm). Other samples also contain a large amount of interstitial materials (matrix content more than 15%) and thus can be classified as lithic graywackes. All are immature with subangular to subrounded detrital grains, moderately sorted, which also indicates short transport and rapid burial. All also have argillaceous/tuffaceous cements. Notably, the abundant igneous fragments imply their main source was magmatic rocks. On the plot of Qt–F–L (fig. 5A) and Qm–F–Lt (fig. 5B), all the samples fall into the field of recycled orogenic and transitional recycled orogenic, respectively. In summary, these sandstones were deposited near their source area.

U-Pb Isotopic Dating of Detrital Zircons

Zircon data from the Huanggangliang and Linxi formations are shown in supplementary table 1, http://earth.geology.yale.edu/%7eajs/SupplementaryData/2020/Wu. To ensure quality, a few U-Pb analyses showing large variations of signals or large age discordance were discarded as explained below. We used $^{206}Pb/^{238}U$ ages for zircons with ages of <1000 Ma and $^{207}Pb/^{206}Pb$ ages for zircons older than 1000 Ma.

Sample of the Huanggangliang Formation

Ninety-five zircon grains from the Huanggangliang Formation sandstone sample 18CFL01 were chosen for U-Pb isotopic dating. The zircon grains are subhedral to euhedral in shape and range from 80 to 200 μm in size. Most of these zircons have oscillatory zoning in CL images (fig. 6A) with high Th/U ratios (0.11–4.29) and only 3 grains have ratios below 0.1. The former indicate a magmatic origin. The zircons show a wide range of concordant ages (figs. 7 and 8A). The detrital zircon ages range from 2653 to 265 Ma, but a dominant group of zircon ages are distributed between 500 Ma and 370 Ma. The histogram (fig. 8A) shows three main age populations: (1) 265 to 488 Ma (n = 64), with a significant peak at ~442 Ma; (2) 1764 Ma to 1935 Ma (n = 10), with an age peak at ~1863 Ma; (3) 2443 to 2653 Ma (n = 14), with an age peak at ~2538 Ma. In addition, two concordant analyses record the youngest ages of 265 Ma and 266 Ma.

Samples of the Linxi Formation

One hundred and one zircon grains from the Linxi Formation sandstone sample 18CFL02 were chosen for U-Pb isotopic dating and 93 zircons are concordant (fig. 7). Zircon grains range from 50 to 150 μm in size and exhibit a primary subhedral to euhedral shape (fig. 6B). Nearly all of the zircons have oscillatory zoning (fig. 6B), indicating their magmatic origin, as does their high Th/U ratios (0.14–2.83), with only 3 grains below 0.1. The SHRIMP U-Pb ages span from 3363 to 263 Ma and cluster around two main populations on a normalized probability plot: 413 to 263 Ma (n = 31) and 571 to 430 Ma (n = 28), with age peaks at ~274 Ma and ~448 Ma, respectively. In addition, detrital zircons with ages greater than 1000 Ma yielded abundant $^{207}Pb/^{206}Pb$ ages from 3363 to 908 Ma (n = 33), showing two age peaks at ~2511 Ma and ~1844 Ma, respectively.

Eighty-two zircon grains from sample 18CFL04 were chosen for U-Pb isotopic dating and 5 were discarded because of high discordance (fig. 7). Similar to sample 18CFL02, zircon grains range from 50 to 150 μm in size and exhibit a primary subhedral to euhedral shape (fig. 6C). CL imaging reveals that most grains have oscillatory zoning (fig. 6C), indicating their magmatic origin, as does high Th/U ratios (0.11–1.35), with only one grain below 0.1. The detrital zircon ages range from 2584 to 257 Ma (fig. 8C), and zircon ages are mostly in the group of 257 to 320 Ma (n = 23) and 413–535 Ma (n = 14), with age peaks at ~276 Ma and ~424 Ma, respectively. Forty Proterozoic zircons yield ages from 859 Ma to 2584 Ma, with age peaks at ~1574 Ma, ~1923 Ma and ~2525 Ma, respectively.

One hundred zircon grains from sample 18CFL05 were chosen for U-Pb isotopic dating and 5 were discarded because of high discordance (fig. 7). Zircon grains are subhedral to euhedral in shape and range from 100 to 200 μm in size; they also exhibit magmatic oscillatory zoning in CL images (fig. 6D), indicating their magmatic origin, as does their high Th/U ratios (0.11–1.63), with only one grain below 0.1. These grains yielded U-Pb ages (fig. 8D) ranging from 3041 Ma to 260 Ma, with major age populations between 387 and 260 Ma (n = 15), 511 to 404 Ma (n = 25), 2189 to 1425 Ma (n = 34), and 3041 to 2263 Ma (n = 13). The youngest detrital zircon age is 260 ± 3 Ma.

Sample 18CFL03 is a tuffaceous pyroclastic rock. Nineteen zircons were chosen for U-Pb isotopic dating, and fifteen zircons are concordant. These zircon grains are generally stubby to elongate and range from 80 to 200 μm in size and exhibit oscillatory zoning in CL images (fig. 6E). Th/U ratios range from 0.36 to 0.71, with an average value of 0.55. We conclude that these analyzed zircons are of magmatic origin. The zircons are predominantly late Paleozoic in age (254–259 Ma) and yielded several older zircon grains (2536 ± 13 Ma; 438 ± 4 Ma; 283 ± 2 Ma; 275 ± 3 Ma). The older zircon grains are considered to be xenocrysts captured either from the nearby Permian volcanic arc rocks or sedimentary rock debris (fig. 6E 4.1, 5.1) during magma ascent. Therefore, these ages are not considered in the calculation of the weighted mean average age. Zircon grains yield a weighted mean $^{206}Pb/^{238}U$ age of 256.7 ± 1.1

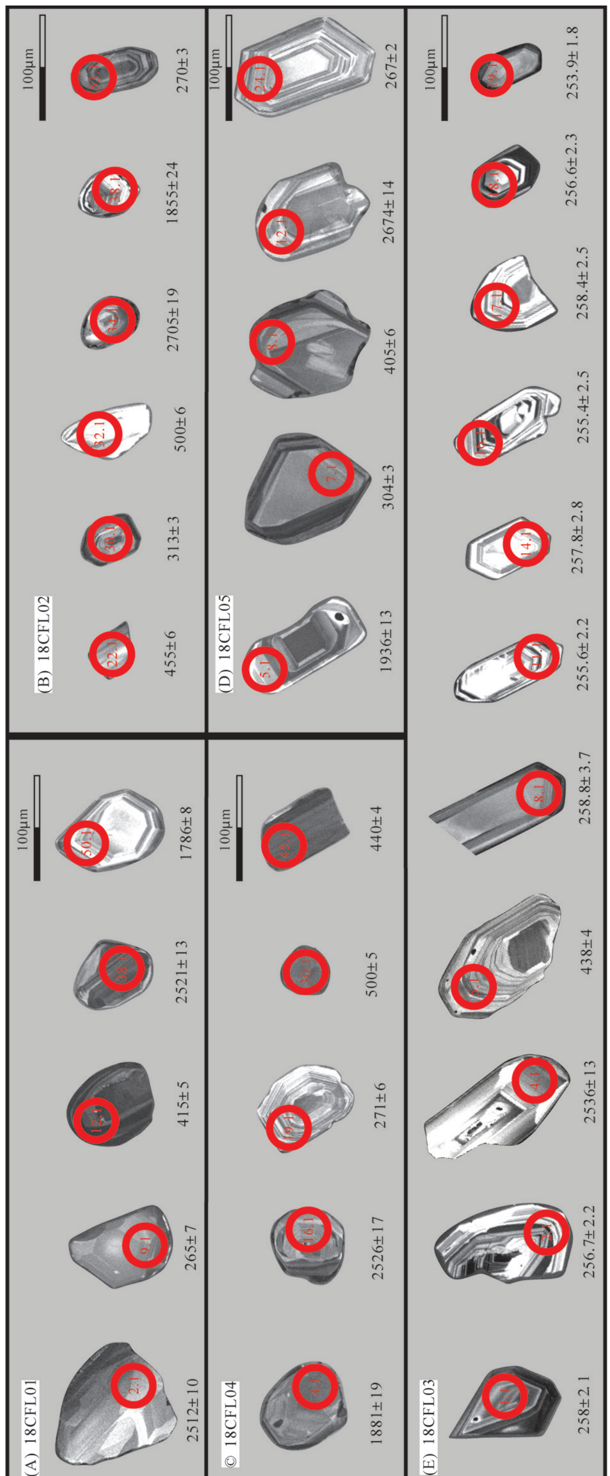

Fig. 6. CL images of representative zircons from the Huangganliang and Linxi formations. The circles represent SHRIMP U-Pb analytical sites. (A) Sample 18CFL01; (B) Sample 18CFL02; (C) Sample 18CFL04; (D) Sample 18CFL05; (E) Sample 18CFL03.

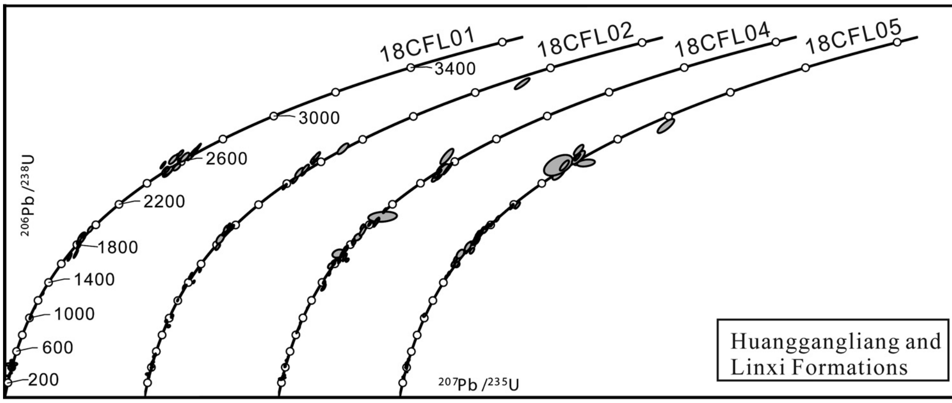

Fig. 7. Zircon U-Pb concordia diagrams for detrital zircons collected from the Huanggangliang and Linxi Formations.

Ma (MSWD = 2.1; fig. 11), which is similar to the youngest zircon age for the Linxi Formation obtained in this paper.

In general, most zircons from all samples show magmatic oscillatory zoning, though a small number of grains underwent metamorphic growth either as single zircons or as rims (fig. 6). All Th/U ratios range from 0.01 to 4.29, with most above 0.1. Most zircons are subhedral to euhedral in shape, with slight abrasion, suggesting that the source rocks were relatively close and had undergone short-distance transportation. These indicate that most zircons from the samples are of magmatic origin and are not far traveled.

DISCUSSION

The Depositional Age of Huanggangliang and Linxi Formations

The depositional age of the Huanggangliang Formation along the Xar Moron River area had been estimated to be middle Permian based on fossils and correlations with fossil-bearing sections (BGMRIM, 1991), which is indeed an effective method. However, the method of isotopic dating provides a more reliable constraint on the maximum depositional age for the strata. The youngest zircon in this study is 265 ± 7 Ma in the Huanggangliang Formation, which together with fossils (BGMRIM, 1991), confirms that its deposition age was middle Permian. In addition, an undeformed felsic dike intrudes the Huanggangliang Formation between the Early Triassic and Middle Triassic, meaning its deposition age is older than the Early Triassic (242 ± 3 Ma; Eizenhöfer and others, 2014). Furthermore, we summarized already published detrital zircon data of Huanggangliang Formation, with a dominant single age peak ranging from 246 Ma to 279 Ma (supplementary table 2, http://earth.geology.yale.edu/%7eajs/SupplementaryData/2020/Wu), yielding a weighted mean age of 265.7 ± 1.5 Ma (MSWD = 2; fig. 9), which is basically consistent with the two youngest zircons (265 Ma and 266 Ma) we obtained from the Huanggangliang Formation. Therefore, we conclude that the Huanggangliang Formation was deposited in the middle Permian.

We found that the youngest age of sample 18CFL04 from Linxi Formation to be 257 ± 8 Ma, which suggests the Linxi Formation probably was deposited after that time. In addition, the weighted mean $^{206}Pb/^{238}U$ ages of eleven zircons from the volcaniclastic unit is 256.7 ± 1.1 Ma (fig. 10), which is coeval with that of the youngest detrital zircon ages from the Linxi Formation and previous studies

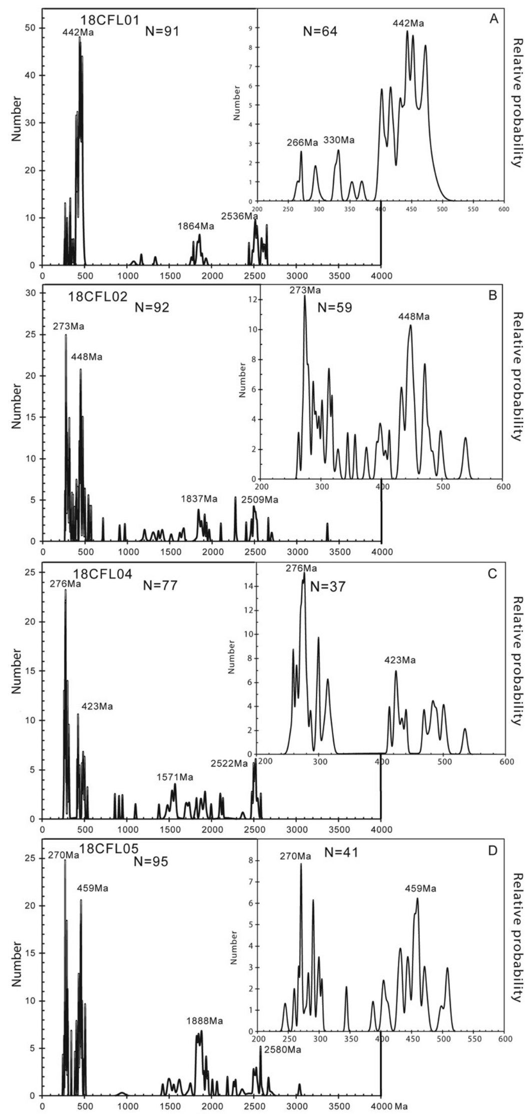

Fig. 8. Age distribution diagram for the Huanggangliang and Linxi formations in the Xar Moron River region. The bottom right inset figures within each U-Pb Concordia diagram are histograms of the Paleozoic zircons.

(Eizenhöfer and others, 2014; Han and others, 2015), suggesting that the Linxi Formation was mainly deposited during the late Permian. Eizenhöfer and others (2014) presented the youngest zircon age of 253 ± 3 Ma from the Linxi Formation on the north side of the Xar Moron River. Also the youngest reported zircon age is ~255 Ma in the Linxi area (Han and others, 2015). Along with our new results, we conclude that the depositional age of the Linxi Formation was late Permian.

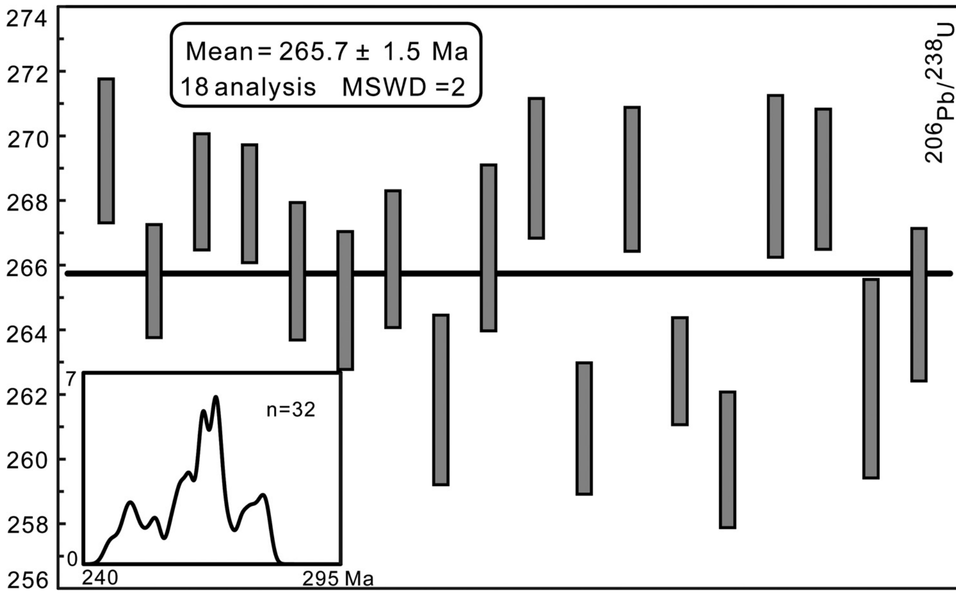

Fig. 9. Plot of weighted mean $^{206}Pb/^{238}U$ age of the Huanggangliang Formation.

Overview of Zircon U-Pb Ages from Potential Source Terranes

In this section, previously published detrital zircon U-Pb ages of Permian strata from adjacent terranes with potential affinities, including NCC, NOB, SOB and the Mongolian microcontinent (fig. 11) are reviewed. Other provenance terranes such as the SC and the Tarim Craton due to their far geographic locations were less likely to have contributed to the sedimentary system in the study region and are excluded from further mention.

The North China Craton

The NCC is one of the main tectonic elements of the Asian tectonic collage, which is characterized by significant magmatic and metamorphic rocks of ~1.85 Ga and ~2.5 Ga (fig. 11A, Zhao and others, 2002; Zhao and others, 2005; Zhai and

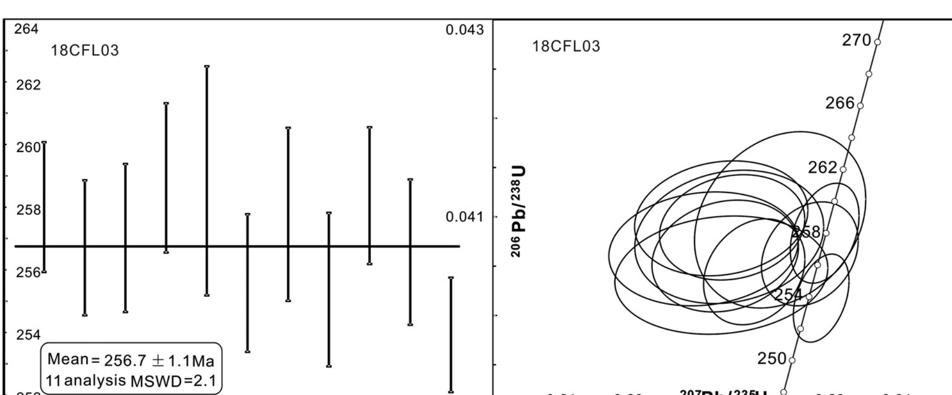

Fig. 10. Plot of weighted mean $^{206}Pb/^{238}U$ age of the tuffaceous pyroclastic rock.

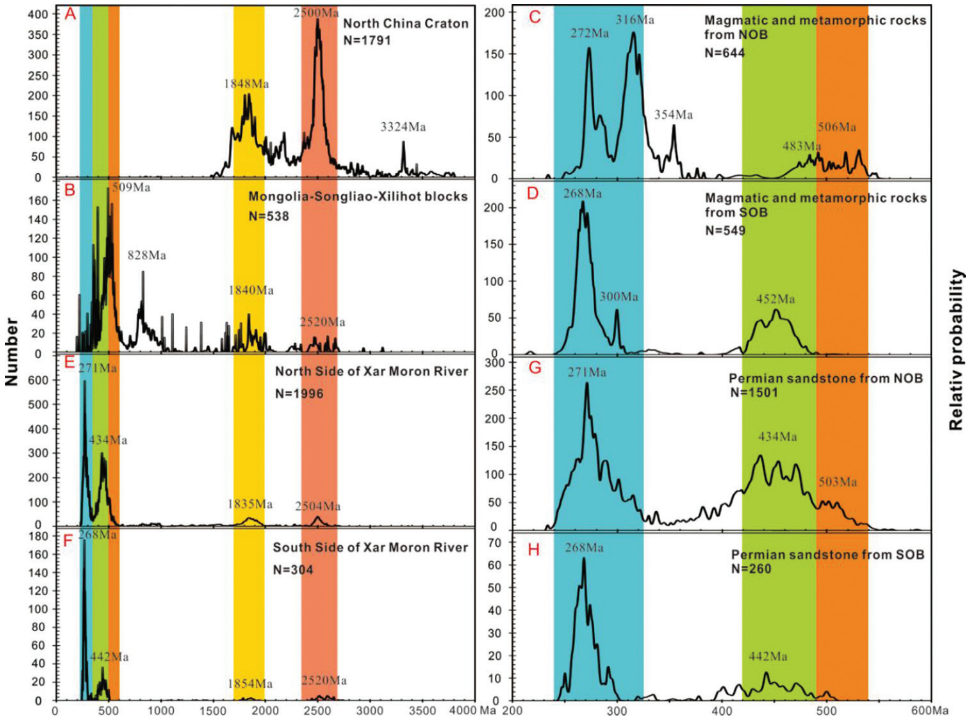

Fig. 11. Comparison of the age population of the Permian sandstones in the Xar Moron River region with those of surrounding major regional provenance terranes: (A) from the NCC (data from Rojas-Agramonte and others, 2011), (B) from Mongolia microcontinent and Songliao-Xilihot blocks (Rojas-Agramonte and others 2011; Li and others, 2011; Sun and others, 2013), (C) from the Paleozoic magmatic rocks in the NOB (data from Shi and others, 2004; Bao and others, 2007; Zhang and others, 2008; Liu and others, 2012; Xu and others, 2012; Li and others, 2014; Li and others, 2015; Hu and others, 2015; Li and others, 2016; Yang and others, 2016; Zhu and others, 2016a; Zhu and others, 2016b; Kong and others, 2017) (D) from the Paleozoic magmatic rocks in the SOB (data from Fan and others, 2009; Li and others, 2010; Zhao and others, 2011; Li and others, 2012; Lu and others, 2012; Wang and others, 2013; Luo and others, 2013; Feng and others, 2013; Zhang and others, 2013; Zhang and others, 2014b; Zhang and others, 2016; Li and others, 2016; Xin and others, 2016; Wang and others, 2016; Zhao and others, 2016; Xue and others, 2018), (E) from the Permian sedimentary rocks in the northern Xar Moron River (this study and Han and others, 2012; Eizenhöfer and others, 2014; Chen and others, 2017; Chen and others, 2016; Han and others, 2017, supplementary table 2, http://earth.geology.yale.edu/%7eajs/SupplementaryData/2020/Wu), (F) from the Permian sedimentary rocks in the southern Xar Moron River (this study and Eizenhöfer and others, 2014, supplementary table 2), G and H are from the Paleozoic detrital zircon ages of E and F, respectively. (Color shaded bars show the main ages peaks, and diagrams on the right are enlargements from the diagrams on the left of the populations with ages between 200 and 600 Ma).

others, 2005; Wang and others, 2009; Wang and others, 2010; Piper and others, 2011, fig. 11A). Following its Paleoproterozoic (~1.85 Ga) consolidation, the NCC underwent the final break away from the Columbia supercontinent, with a transition to a Paleo-Asian ocean tectonic collage in the period ~1.32 to 1.35 Ga (Zhang and others, 2009). In addition, Grenvillian (~0.9–1.0 Ga) magmatic, metamorphic events at the northern margin of NCC have been reported (Peng and others, 2011; Fu and others, 2015; Liu and others, 2017b).

The Southern Orogenic Belt

The major tectonic units of the SOB include the Ondor Sum subduction-accretion complex (Hu and others, 1990; Xiao and others, 2003) which contains turbidites, olistostrome mélanges, and blueschists, in a nearly E-W trending ophiolite belt about

200 km long and 25 km wide (Hu and others, 1990). It also includes the Bainaimiao arc that borders the NCC fault (Hu and others, 1990; Johnson and others, 2001). The SOB is characterized by a discontinuous early to late Paleozoic magmatic belt and the overall lithology is dominated by Permian volcanic arc rocks and volcaniclastic sedimentary rocks (BGMRIM, 1991). Abundant early to late Paleozoic ages of magmatic rocks from ~518 to ~240 Ma (fig. 11D) have been reported in this belt (Liu and others, 2003; Jian and others, 2008; Lu and Li, 2009; Li and others, 2010; Tong and others, 2010; Zhang and others, 2013; Zhang and others, 2014b). The Permian sedimentary rocks exposed in the SOB include detrital zircon U-Pb ages clustering at 324 to 245 and 498 to 394 Ma, with significant age peaks at 269 Ma and 442 Ma, respectively (fig. 11F).

The Northern Orogenic Belt

The NOB forms a north-dipping thrust belt consisting, from south to north, of the Xilinhot metamorphic complex (Tang, 1990), the Erdaojing subduction-accretion complex (Xu and Chen, 1997), and the Baiyanbaolidao pluton (Chen and others, 2000; Jian and others, 2008), extending over 1000 km from east to west. In recent years, based on these data, reported data for the metamorphic basement constituents, cover sequences, and formation ages in different blocks, Liu and others (2017a) proposed that the Paleozoic tectonic divisions are, from west to east, the Erguna block, the Xing'an block, the Songliao-Xilinhot block and the Jiamusi block. The NOB is characterized by sporadically exposed early to mid-Paleozoic magmatic rocks and ~500 Ma Pan-African metamorphic rocks (Jian and others, 2008; Zhou and others, 2012) and the lithology is dominated by late Paleozoic volcanic arc rocks and volcaniclastic strata (BGMRIM, 1991). Early to late Paleozoic magmatic rocks are widely distributed in this belt, with ages of ~500 to ~250 Ma (fig. 11C, Xiao and others, 2003; Shi and others, 2004; Zhang and others, 2008; Miao and others, 2008; Wilde and others, 2010; Tang and others, 2011; Zhou and others, 2012; Chen and others, 2014; Hu and others, 2015). The Permian sedimentary rocks in this belt are dominated by the 350 to 238, 544 to 350, 1970 to 1750 and 2650 to 2400 Ma age populations and other sporadically distributed detrital zircons from 1640 to 650 Ma (fig. 11E). Although the U-Pb age spectrum of zircons in the NOB displays very similar detrital zircon U-Pb ages with those of the SOB, the former have an abundant Pan-African ages with an age peak at ~500 Ma, which is related to the Pan-African orogenic event. For example, Zhou and others (2012) proposed that the Songliao block in the NOB has Pan-African basement and represents fragments that rifted from northern Gondwana.

The Mongolia-Songliao-Xilinhot Block

The Mongolian arcs extend along the northern margin of Chinese Inner Mongolia and represent an assemblage of Paleozoic arcs and Precambrian microcontinents which successively were accreted onto the SC during the subduction of the PAO (Badarch and others, 2002; Xiao and others, 2003; Windley and others, 2007). Formation ages for the Mongolian microcontinent range from the Paleoproterozoic to late Paleozoic and have detrital zircon U-Pb ages clustering at 600 to 350 Ma, 1020 to 700 Ma and 2570–1240 Ma (Rojas-Agramonte and others, 2011). The Songliao-Xilinhot block is located in central NE China and mainly covered by the Songliao Basin, and consists of two sub-blocks (the Songliao and Xilinhot blocks). Considered from the geotectonic view, the Mongolia-Songliao-Xilinhot block is located in the NOB, so we regard it as part of the NOB (fig. 1B). The Mongolian-Songliao-Xilinhot block is characterized by preponderantly Pan-African ages with an age peak at ~509 Ma (fig. 11B), displaying very similar detrital zircon U-Pb age spectra with those of the NOB.

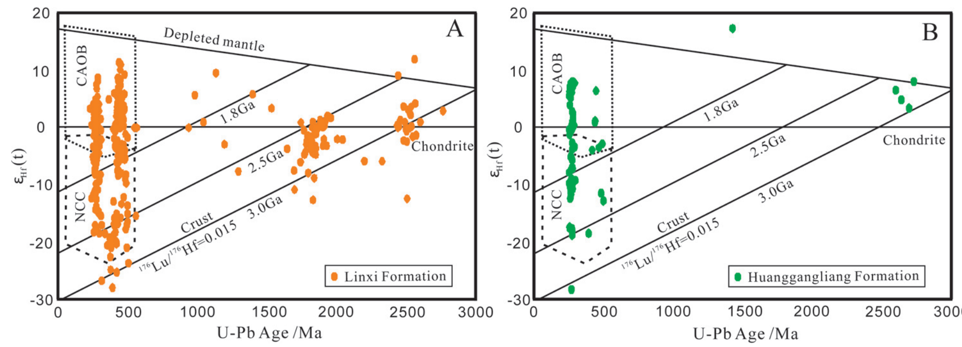

Fig. 12. Plots of detrital zircon εHf(t) values vs. U-Pb ages for Permian sandstones. (A) Linxi Formation; (B) Huanggangliang Formation (data from Eizenhöfer and others, 2018).

Provenance Analysis and Implications for Tectonic Evolution Provenance of the Huanggangliang and Linxi Formations

The Permian sandstones in both formations show sub-rounded shapes with poor sorting and low maturation of texture and components, indicating short transport and rapid accumulation. In addition, their abundant lithic fragments (mainly volcanic, fig. 4, table 1) show that their provenance was mainly magmatic rocks, which is consistent with the moderate to high Th/U ratios of detrital zircons. The petrography analysis results suggest that the provenance of the Permian sandstones in both formation was mainly from an arc collision-orogenic belt. The NOB and SOB with abundant magmatic rocks are clearly the provenance of these Permian sandstones.

A total of 308 detrital zircon U-Pb ages were compiled from the Huanggangliang Formation and they show four main age clusters at 330 to 220 Ma, 500 to 370 Ma, 1920 to 1760 Ma, 2660 to 2400 Ma and without distinct age peaks between 1700 and 500 Ma. In addition, the collected samples from the Zhesi and Linxi formations yielded detrital zircon U-Pb ages ranging from 3400 Ma to 230 Ma, with four age clusters: at 350 to 230 Ma, 540 to 360 Ma, 2000 to 1700 Ma, 2600 to 2400 Ma and a broad peak from 1600 and 700 Ma without other pronounced age peaks (figs. 11E and 11F). Such age spectra of detrital zircons with ages of 350 to 220 Ma and 540 to 360 Ma in the study area indicate that early and late Paleozoic rocks were their predominant source. The NOB and SOB, both characterized by early to late Paleozoic magmatic rocks (for example: Xiao and others, 2003; Shi and others, 2004; Jian and others, 2008; Zhang and others, 2013) are the most potential source terranes. In addition, Hf isotopic data of Permian sedimentary sandstones of the Linxi and Huanggangliang formations (supplementary table 3, http://earth.geology.yale.edu/%7eajs/SupplementaryData/2020/Wu) were taken from Eizenhöfer and others (2018) with their ε_{Hf} values mostly ranging from ~-20 to ~+15. The plots of ε_{Hf} (t) values vs. U-Pb ages (fig. 12, supplementary table 3, http://earth.geology.yale.edu/%7eajs/SupplementaryData/2020/Wu) for sandstones of the Huanggangliang and Linxi formations further support that the NOB and SOB were their major provenance (figs. 11A and 11B). However, their contribution to the early and late Paleozoic age population of Permian sedimentary rocks would be indistinguishable.

South of the Xar Moron River, samples collected from the Huanggangliang Formation exhibit a simple zircon age spectrum (figs. 11F and 11H). The age spectrum for the southern samples is similar in the NOB (fig. 11C) and the SOB (fig. 11D), so we cannot discriminate which was their provenance according to age comparison. The absence of Pan-African age populations and Neoproterozoic zircons

(~1000–700 Ma) and the U-Pb age spectra of samples from south of Xar Moron River further support the differences in provenance on either side of the Xar Moron River, (fig. 11F). Precambrian zircon age populations of ~2000–1700 Ma and ~2660 to 2400 Ma occur in all samples. Although ~1800 Ma and ~2500 detrital zircons occur both in the NCC and NOB, the ~500 Ma metamorphic event did not take place in the NCC (Rojas-Agramonte and others, 2011). The specific peak age of ~503 Ma is quite different from that of the NCC (fig. 11A) and more Neoproterozoic zircons (~1000–700 Ma) were present in the samples collected in the north than in those collected in the south. Therefore, we can use the difference between them as a breakthrough for provenance analysis. Moreover, the ε_{Hf} values for the ~1800 Ma and 2500 Ma zircons are consistent with those reported for the NCC, indicating minor provenance from the NCC.

To the north, complex patterns were found in the zircon age spectra of the collected samples. This indicates that in exposed tectonic units, the zircon age spectra are different from each other and the provenance became more complex compared to those from south of the Xar Moron River. The Archean to Paleoproterozoic age peaks (~2504 Ma and ~1835 Ma) detected north of the Xar Moron River are similar to those from the NOB and NCC (figs. 11A and 11B), with positive ε_{Hf} (t) values. A few zircons plot in the NCC field of ε_{Hf} (t) values vs. U-Pb ages, suggesting a provenance component from the south of the study area (NCC). The negative ε_{Hf} (t) values yielded by some Paleozoic zircons display stronger shifts toward positive ε_{Hf} values, which may indicate crustal reworking of this block (fig. 12). Notably, the range of 540 to 490 Ma with a peak at 503 Ma yielded by the northern samples (fig. 11G) could also be found in the NOB and Mongolian micro-continent (Rojas-Agramonte and others, 2011; Zhou and others, 2012), but not the NCC. Hence, the NOB has obvious Pan-African ages relative to the SOB, which is important to distinguish the provenance of Permian sandstones on both sides of the Xar Moron River. However, Pan-African ages were reported in the early Paleozoic metamorphosed sedimentary rocks from the Bainaimiao arc belt in the SOB (Zhang and others, 2014c). Assuming that provenance of the samples from the NCC and the SOB, the Pan-African zircons (540–490 Ma with a peak at 503 Ma) and Neoproterozoic zircons (~1000– ~700 Ma) from the Zhesi Formation come from the SOB, then, these two age populations should also have occurred in the southern samples from the Huanggangliang Formation (equivalent Permian strata to the north of the Xar Moron River are called the Zhesi Formation), but this is not the case. The absence of Pan-African and Neoproterozoic zircons in the northern samples suggests that the zircon ages of Permian sedimentary rocks collected on both sides of the Xar Moron River may have different material sources. Furthermore, Chen and others (2015) obtained southward paleocurrents from the Zhesi Formation to the north of Solonker Suture Zone, which offers evidence of a northern provenance. The Neoproterozoic zircons (~1000–700 Ma) detected in the samples from the northern margin of the river were likely derived from the Xilinhot block (Li and others, 2011; Sun and others, 2013). Thus, we speculate that the provenance of the samples from north of the Xar Moron River may have come from the NOB and were mixed with a small amount of NCC material.

In summary, the zircon ages of Permian sedimentary rocks collected on both sides of the Xar Moron River show significant differences: the northern samples have abundant Pan-African zircon ages, together with Neoproterozoic zircons, while the samples from south of the river lack these two characteristic age populations. Hence, we conclude that the provenance of the Permian sedimentary rocks from the northern margin of the Xar Moron River was Mongolia, NOB and a small amount of Mesoproterozoic-Paleoproterozoic zircons may be from the NCC. We also conclude that the early and late Paleozoic zircons from the southern margin originated mostly from the SOB and also that a number of Precambrian zircons may also have been contributed by the NCC.

Implications for the Tectonic Evolution of the Eastern Segment of the CAOB

The location of the final collision of the North China and Siberia cratons is controversial. Some workers proposed that the final suture of the PAO was along the Heihe-Hegenshan belt (Tang, 1990; Miao and others, 2007; Miao and others, 2008). However, most scholars strongly support that the Solonker-Xar Moron-Changchun-Yanji belt was the final closure suture of the PAO based on tectonic, magmatic petrology, and sedimentology observations (Xiao and others, 2003; Li and others, 2006; Wu and others, 2007a; Xiao and others, 2009; Jian and others, 2010; Liu and others, 2010; Sun and others, 2013; Xiao and others, 2015; Han and others, 2015). In addition, this view is supported by discontinuous outcropping of ophiolites, syn-collisional granites, radiolarian cherts and strongly deformed rocks along the suture (Sun and others, 2004; Li and others, 2007; Wu and others, 2007b).

Detrital zircon age spectra of sandstones derived from magmatic rocks record surrounding magmatic events (Hawkesworth and others, 2010). The samples of sedimentary rocks on both sides of the Xar Moron River have age populations of early Paleozoic and late Paleozoic (figs. 11G and 11H), which indicate the existence of at least two main periods of magmatism in this area. The early Paleozoic age groups from both sides of the Xar Moron River with significant peaks at ~434 Ma and 442 Ma, respectively (figs. 11G and 11H), are consistent with the ages of the early Paleozoic subduction-collision related magmatic rocks that outcrop in the NOB and SOB (Jian and others, 2008; Zhang and others, 2013; Zhang and others, 2014a). In the early to middle Permian, extensive extension took place in the northern continental block, while the southern continental block showed strong subduction with consumption of a ridge-trench system (Jian and others, 2010). This is consistent with a large number of late Paleozoic detrital zircons recorded from two sides of the Xar Moron River. To the north of Sonid Left Banner, there are abundant alkaline granitic magmatic rocks (Hong and others, 1994). There are also widespread rift-related bimodal volcanic rocks in the Xi Ujimqin Banner (Zhang and others, 2008), which are concluded to be the products of asthenosphere upwelling and underplating. Abundant early to middle Permian magmas and volcanics were intruded and erupted, respectively, along the near east-west-trending midline of the NOB and were added to the source of the upper Linxi Formation.

The age of ophiolites between the Hegenshan and the Ondor Sum-Xar Moron suture zones (Miao and others, 2007; Miao and others, 2008) implies that the PAO was still in a narrow ocean setting. In addition, Shang (2004) made a detailed survey of the paleontology of Permian deep marine strata which confirmed that the PAO still existed during the Guadalupian period and at least during this period, some deep basinal sedimentation occurred. Interestingly, Zhang and others (2014a) found large numbers of bryozoan and sponge spicule fossils in the thick limestone layers and lenses of the upper part of the Linxi Formation in the Guandi section of Linxi County in eastern Inner Mongolia, thus suggesting that the sedimentary environment was a shallow sea. As we have discussed above, the Permian sedimentary rocks on both sides of the Xar Moron River have obviously different provenance, suggesting that there was a wide and deep ocean between them during the Permian, possibly the PAO. The Permian sedimentary rocks from the northern margin of the river have NOB and Mongolian micro-continent affinity. However, the age spectrum from the southern margin samples are consistent with the recent report of Chen and others (2016), who consider that their provenance is related to the SOB and the NCC. Furthermore, our age results imply that the provenance of sandstones from the Linxi Formation on the north side of the Xar Moron River may have been derived from the basement rocks of NCC, which may indicate the onset of the final collision between the northern margin of the NCC and the SC. Therefore, an ocean existed during the late Permian according to the evidence above and the sedimentary rocks of the Linxi Formation that were deposited during this period. The final collision is concluded to be located in the Solonker-Mandula-Xar Moron area, which extends from the Solonker eastwards through the Mandula area, the Xar Moron river, through central Jilin Province to the Yanji area and marks the final collision zone between the two active continental margins of the Siberian and North China cratons. Soon after entering the post-collision stage at the northern margin of the NCC, the PAO closed. Recently, more and more post-collisional granites have been reported in central Inner Mongolia (Li and others, 2007; Shi and others, 2007; Lian and others, 2021) suggesting that the eastern segment of the CAOB went into post-orogenic extension.

CONCLUSIONS

Based on a systematic SHRIMP U-Pb isotopic study of detrital zircons and petrographic analysis of Permian sedimentary rocks on the northern and southern margins of the Xar Moron River, and previous studies, we offer the following conclusions:

We conclude that the deposition of the Linxi Formation occurred in the late Permian, based on the tuffaceous pyroclastic sediment with a weighted mean $^{206}Pb/^{238}U$ age of 256.7 ± 1.1 Ma (MSDW = 2.1, n = 11). Sandstone provenance is concluded to have come from recycled orogenic material and underwent short distance transportation. The age spectrum of the Permian sandstones in the northern of Xar Moron River is similar to the Northern Orogenic Belt and Mongolia microcontinent. However, the age spectrum of Permian sandstones in the southern margin of the river is similar to the SOB and NCC. In the Middle Permian and before, there was no mixing of provenance on both sides. Until the deposition of the Linxi Formation, a small amount of basement material from the NCC came to the opposite bank, indicating that the PAO had closed. These observations indicate that the Xar Moron River fault zone is the final collision zone of the eastern segment of the CAOB and the final closure of the eastern segment of the PAO occurred during late Permian-earliest Triassic times.

ACKNOWLEDGMENTS

This study was encouraged by Professor A. Kröner, who has made outstanding achievements in geology all his life. We really appreciate Professor Kröner for his great suggestions in our research. We would like to commemorate him with this article. This paper was significantly improved by comments from Guest Editor Guochun Zhao, Professors Shuanhong Zhang, Chaohui Liu, and the other anonymous reviewers. We would like to thank Zemin Bao and other members of the Beijing SHRIMP Center for helping with SHRIMP analysis, and we also thank Linlin Li, Yuelan Kang and Zhen Wang for their help in field sampling and sample analysis. This study was financially supported by the National Natural Science Foundation of China (Grant no. 41872209), the Geological Survey of China (Grant no. DD20190004), China National Space Administration (Grant No. D020205), and the CGS Research Fund (Grant no. JYYWF20180104).

REFERENCES

Badarch, G., Cunningham, W. D., and Windley, B. F., 2002, A new terrane subdivision for Mongolia: Implications for the Phanerozoic crustal growth of Central Asia: Journal of Asian Earth Sciences, v. 21, n. 1, p. 87–110, https://doi.org/10.1016/S1367-9120(02)00017-2

Bao, Q. Z., Zhang, C. J., Wu, Z. L., Wang, H., Li, W., Sang, J. H., and Liu, Y. S., 2007, Zircon SHRIMP U-Pb dating of granitoids in a Late Paleozoic rift area, southeastern Inner Mongolia, and its implications: Geology in China, v. 34, p. 790–798 (in Chinese with English abstract).

Black, L. P., Kamo, S. L., Allen, C. M., Aleinikoff, J. N., Davis, D. W., Korsch, R. J., and Foudoulis, C., 2003, TEMORA 1: A new zircon standard for Phanerozoic U-Pb geochronology: Chemical Geology, v. 200, n. 1–2, p. 155–170, https://doi.org/10.1016/S0009-2541(03)00165-7

BGMRIM, 1991, Bureau of Geology and Mineral Resources of Inner Mongolia, Regional geology of Nei Mongol (Inner Mongolia) Autonomous Region: Beijing, China, Geological Publishing House, v. 25, p. 1–725 (in Chinese with English summary).

Cawood, P. A., and Nemchin, A. A., 1999, U-Pb dating of detrital zircons: Implications for the provenance record of Gondwana margin terranes: GSA Bulletin: v. 111, n. 8, p. 1107–1119, https://doi.org/10.1130/0016-7606(1999)111<1107:UPDODZ>2.3.CO;2

Chen, B., Jahn, B. M., Wilde, S., and Xu, B., 2000, Two contrasting Paleozoic magmatic belts in northern Inner Mongolia, China: Petrogenesis and tectonic implications: Tectonophysics, v. 328, n. 1–2, p. 157–182, https://doi.org/10.1016/S0040-1951(00)00182-7

Chen, Y., Zhang, Z. C., Li, K., Luo, Z. W., Tang, W. H., and Li, Q. G., 2014, Geochronology, geochemistry and geological significance of the Permian bimodal volcanic rocks in Xi Ujimqin Banner, Inner Mongolia: Acta Scientiarum Naturalium Universitatis Pekinensis, v. 50, p. 843–858 (in Chinese with English abstract), http://www.oaj.pku.edu.cn/wk3/syxk/EN/

Chen, Y., Zhang, Z. C., Li, K., Yu, H. F., and Wu, T. R., 2016, Detrital zircon U–Pb ages and Hf isotopes of Permo-Carboniferous sandstones in central Inner Mongolia, China: Implications for provenance and tectonic evolution of the southeastern Central Asian Orogenic Belt: Tectonophysics, v. 671, p. 183–201, https://doi.org/10.1016/j.tecto.2016.01.018

Cherniak, D. J., and Watson, E. B., 2001, Pb diffusion in zircon: Chemical Geology: Chemical Geology, v. 172, n. 1–2, p. 5–24, https://doi.org/10.1016/S0009-2541(00)00233-3

Dickinson, W. R., 1985, Interpreting Provenance Relations from Detrital Modes of Sandstones, in Zuffa, G. G., editor, Provenance of Arenites: NATO ASI Series, v. 148, p. 333–361

Dickinson, W. R., and Suczek, C. A., 1979, Plate tectonics and sandstone composition: AAPG Bulletin, v. 63, p. 2164–2182, https://doi.org/10.1306/2F9188FB-16CE-11D7-8645000102C1865D

Dickinson, W. R., Beard, L. S., Brakenridge, G. R., Erjavec, J. L., Ferguson, R. C., Inman, K. F., Knepp, R. A., Lindberg, F. A., and Ryberg, P. T., 1983, Provenance of North American Phanerozoic sandstones in relation to tectonic setting: GSA Bulletin, v. 94, n. 2, p. 222–235, https://doi.org/10.1130/0016-7606(1983)94<222:PONAPS>2.0.CO;2

Eizenhöfer, P. R., and Zhao, G. C., 2018, Solonker Suture in East Asia and its bearing on the final closure of the eastern segment of the Palaeo-Asian Ocean: Earth-Science Reviews, v. 186, p. 153–172, https://doi.org/10.1016/j.earscirev.2017.09.010

Eizenhöfer, P. R., Zhao, G. C., Zhang, J., and Sun, M., 2014, Final closure of the Paleo-Asian Ocean along the Solonker Suture Zone: Constraints from geochronological and geochemical data of Permian volcanic and sedimentary rocks: Tectonics, v. 33, n. 4, p. 441–463, https://doi.org/10.1002/2013TC003357

Fan, H. R., Hu, F. F., Yang, K. F., Wang, K. Y., and Liu, Y. S., 2009, Geochronology framework of late Paleozoic dioritic-granitic plutons in the Bayan Obo area, Inner Mongolia, and tectonic significance: Acta Petrologica Sinica, v. 25, n. 11, p. 2933–2938 (in Chinese with English abstract).

Feng, L. X., Zhang, Z. C., Han, B. F., Ren, R., Li, J. F., and Su, L., 2013, LA-ICP-MS zircon U-Pb ages of granitoids in Darhan Muminggan Joint Banner, Inner Mongolia, and their geological significance: Geological Bulletin of China, v. 11, p. 1737–1748 (in Chinese with English abstract).

Fu, X. M., Zhang, S. H., Li, H. Y., Ding, J. K., Li, H. K., Yang, T. S., Wu, H. C., Yuan, H. F., and Lv, J., 2015, New paleomagnetic results from the Huaibei Group and Neoproterozoic mafic sills in the North China Craton and their paleogeographic implications: Precambrian Research, v. 269, p. 90–106, https://doi.org/10.1016/j.precamres.2015.08.013

Han, G.Q., Liu, Y.J., Neubauer, F., Jin, W., Genser, J., Ren, S.M., Li, W., Wen, Q.B., Zhao, Y.L., and Liang, C.Y., 2012, LA-ICP-MS U-Pb dating and Hf isotopic compositions of detrital zircons from the Permian sandstones in Da Xing'an Mountains, NE China: New evidence for the eastern extension of the Erenhot–Hegenshan suture zone: Journal of Asian Earth Sciences, v. 49, n. 2, p. 249–271, https://doi.org/10.1016/j.jseaes.2011.11.011

Han, J., Zhou, J. B., Wang, B., and Cao, J. L., 2015, The final collision of the CAOB: Constraint from the zircon U-Pb dating of the Linxi Formation: Geoscience Frontiers, v. 6, n. 2, p. 211–225, https://doi.org/10.1016/j.gsf.2014.06.003

Han, J., Zhou, J. B., Wilde, S. A., and Song, M. C., 2017, Provenance analysis of the Late Paleozoic sedimentary rocks in the Xilinhot Terrane: Journal of Asian Earth Sciences, v. 144, p. 69–81, https://doi.org/10.1016/j.jseaes.2016.12.003

Han, Y. G., and Zhao, G. C., 2018, Final amalgamation of the Tianshan and Junggar orogenic collage in the southwestern Central Asian Orogenic Belt: Constraints on the closure of the Paleo-Asian Ocean: Earth-Science Reviews, v. 186, p. 129–152, https://doi.org/10.1016/j.earscirev.2017.09.012

Hawkesworth, C., Dhuime, B., Pietranik, A., Cawood, P. A., Kemp, A. I. S., and Storey, C. D., 2010, The generation and evolution of the continental crust: Journal of the Geological Society, v. 167, p. 229–248, https://doi.org/10.1144/0016-76492009-072

Hong, D. W., Huang, H. Z., Xiao, Y. J., Xu, H. M., and Jin, M. Y., 1994, The Permian alkaline granites in central Inner Mongolia and their geodynamic significance: Acta Geological Sinica, v. 68, p. 219–230 (in Chinese with English abstract).

Hu, B., Zhai, M. G., Peng, P., Liu, F., Diwu, C. R., Wang, H. Z., and Zhang, H. D., 2013, Late Paleoproterozoic to Neoproterozoic geological events of the North China Craton: evidences from LA-

ICP-MS U-Pb geochronology of detrital zircons from the Cambrian and Jurassic sedimentary rocks in Western Hills of Beijing: Acta Petrologica Sinica, v. 29, p. 2508–2536 (in Chinese with English abstract).
Hu, C. S., Li, W. B., Xu, C., Zhong, R. C., and Zhu, F., 2015, Geochemistry and zircon U-Pb-Hf isotopes of the granitoids of Baolidao and Halatu plutons in Sonidzuoqi area, Inner Mongolia: Implications for petrogenesis and geodynamic setting: Journal of Asian Earth Sciences, v. 97, Part B, p. 294–306, https://doi.org/10.1016/j.jseaes.2014.07.030
Hu, X., Xu, C., and Niu, S., 1990, Evolution of the Early Paleozoic Continental Margin in Northern Margin of the North China Platform: Beijing, China, Beijing University Press, p. 6–23 (in Chinese with English abstract).
Jahn, B. M., Wu, F. Y., and Chen, B., 2000, Granitoids of the Central Asian Orogenic Belt and continental growth in the Phanerozoic: Earth and Environmental Science Transactions of the Royal Society of Edinburgh Earth Science, v. 91, n. 1–2, p. 81–93, https://doi.org/10.1017/S0263593300007367
Jahn, B. M., Windley, B., Natal'in, B., and Dobretsov, N., 2004, Phanerozoic continental growth in Central Asia: Journal of Asian Earth Sciences, v. 23, n. 5, p. 599–603, https://doi.org/10.1016/S1367-9120(03)00124-X
Jian, P., Liu, D. Y., Kröner, A., Windley, B. F., Shi, Y. R., Zhang, F. Q., Shi, G. H., Miao, L. C., Zhang, W., Zhang, Q., Zhang, L. Q., and Ren, J. S., 2008, Time scale of an early to mid-Paleozoic orogenic cycle of the long-lived Central Asian Orogenic Belt, Inner Mongolia of China: Implications for continental growth: Lithos, v. 101, n. 3–4, p. 233–259, https://doi.org/10.1016/j.lithos.2007.07.005
Jian, P., Liu, D., Kröner, A., Windley, B. F., Shi, Y., Zhang, W., Zhang, F., Miao, L., Zhang, L., and Tomurhuu, D., 2010, Evolution of a Permian intraoceanic arc-trench system in the Solonker suture zone, Central Asian Orogenic Belt, China and Mongolia: Lithos, v. 118, p. 169–190, https://doi.org/10.1016/j.lithos.2010.04.014
Johnson, M. E., Rong, J. Y., Wang, C. Y., and Wang, P., 2001, Continental island from the upper Silurian (Ludfordian Stage) of Inner Mongolia: Implications for eustasy and paleogeography: Geology, v. 29, n. 10, p. 955–958, https://doi.org/10.1130/0091-7613(2001)029<0955:CIFTUS>2.0.CO;2
Kong, L. J., Han, B. F., Zheng, B., Feng, L. X., Wang, Z. Z., and Su, L., 2017, Geochronology, geochemistry and tectonic significances of the granites to the northeast of Erenhot, Inner Mongolia: Acta Petrologica et Mineralogica, v. 36, n. 4, p. 433–457.
Kosler, J., and Sylvester, P. J., 2003, Present trends and the future of zircon in geochronology: Laser ablation ICP-MS, *in* Hanchar, J. M., and Hoskin, P. M. O., editors: Reviews in Mineralogy and Geochemistry, v. 53, p. 243–275, https://doi.org/10.2113/0530243
Krogh, T. E., and Keppie, J. D., 1990, Age of detrital zircon and titanite in the Meguma Group, southern Nova Scotia, Canada: Clues to the origin of the Meguma Terrane: Tectonophysics, v. 177, n. 1–3, p. 302–323, https://doi.org/10.1016/0040-1951(90)90287-I
Kröner, A., Windley, B. F., Badarch, G., Tomurtogoo, O., Hegner, E., Jahn, B. M., Gruschka, S., Khain, E. V., Demoux, A., and Wingate, M. T. D., 2007, Accretionary growth and crust-formation in the central Asian Orogenic Belt and comparison with the Arabian-Nubian shield, *in* Hatcher, R. D. Jr., Carlson, M. P., McBride, J. H., and Catalan, J. R., editors, The 4-D Framework of the Continental Crust-Integrating Crustal Processes through Time: Geological Society of America Memoir, v. 200, p. 181–209, https://doi.org/10.1130/2007.1200(11)
Kröner, A., Lehmann, J., Schulmann, K., Demoux, A., Lexa, O., Tomurhuu, D., Stipska, P., Liu, D., and Wingate, M. T. D., 2010, Lithostratigraphic and geochronological constraints on the evolution of the Central Asian Orogenic Belt in SW Mongolia: Early Paleozoic rifting followed by late Paleozoic accretion: American Journal of Science, v. 310, n. 7, p. 523–574, https://doi.org/10.2475/07.2010.01
Kröner, A., Kovach, V. P., Kozakov, I. K., Kirnozova, T., Azimov, P., Wong, J., and Geng, H. Y., 2015, Zircon ages and Nd-Hf isotopes in UHT granulites of the Ider Complex: A cratonic terrane within the Central Asian Orogenic Belt in NW Mongolia: Gondwana Research, v. 27, n. 4, p. 1392–1406, https://doi.org/10.1016/j.gr.2014.03.005
Lee, J. K. W., Williams, I. S., and Ellis, D. J., 1997, Pb, U and Th diffusion in natural zircon: Nature, v. 390, p. 159–162, https://doi.org/10.1038/36554
Li, F. L., Qu, X. Y., Liu, L., Yang, D. M., Wang, D. H., and Zhao, G. X., 2009, Sedimentary Environment on Upper Permian Linxi Group in Inner Mongolia: Acta Sedimentologica Sinica, v. 27, n. 3, p. 265–272 (in Chinese with English abstract).
Li, J. F., Zhang, Z. C., and Han, B. F., 2010, Ar-Ar and zircon SHRIMP geochronology of hornblendite and diorite in northern Darhan Muminggan Joint Banner, Inner Mongolia, and its geological significance: Acta Mineralogica et Petrologica, v. 29, n. 6, p. 732–740 (in Chinese with English abstract).
Li, J. Y., 2006, Permian geodynamic setting of Northeast China and adjacent regions: Closure of the Paleo-Asian Ocean and subduction of the Paleo-Pacific Plate: Journal of Asian Earth Sciences, v. 26, n. 3–4, p. 207–224, https://doi.org/10.1016/j.jseaes.2005.09.001
Li, J. Y., Gao, L. M., Sun, G. H., Li, Y. P., and Wang, Y. B., 2007, Shuangjingzi middle Triassic syncollisional crust-derived granite in the east Inner Mongolia and its constraint on the timing of collision between Siberian and Sino-Korean Paleo-plates: Acta Petrologica Sinica, v. 23, n. 3, p. 565–582 (in Chinese with English abstract).
Li, J. Y., Qu, J. F., Zhang, J., Liu, J. F., Xu, W. L., Zhang, S. H., Guo, R. Q., Zhu, Z. X., Li, Y. P., Li, Y. F., Wang, T., Xu, X. Y., Li, Z. P., Liu, Y. Q., Sun, L. X., Jian, P., Zhang, Y., Wang, L. J., Peng, S. H., Feng, Q. W., Wang, Y., Wang, H. B., and Zhang, X. X., 2013, New Developments on the reconstruction of Phanerozoic geological history and research of metallogenic geological settings of the Northern China Orogenic Region: Geological Bulletin of China, v. 32, p. 207–219 (in Chinese with English abstract).
Li, K., Zhang, Z. C., Feng, Z. S., Li, J. F., Tang, W. H., and Luo, Z. W., 2014, Zircon SHRIMP U-Pb dating and its geological significance of the Late-Carboniferous to Early-Permian volcanic rocks in Bayanwula

area, the central of Inner Mongolia: Acta Petrologica Sinica, v. 30, n. 7, p. 2041–2054 (in Chinese with English Abstract.
Li, K., Zhang, Z. C., Feng, Z. S., Li, J. F., Tang, W. H., Luo, Z. W., and C., Y., 2015, Two-Phase Magmatic Events during Late Paleozoic in the North of the Central Inner Mongolia-Da Hinggan Orogenic Belt and Its Tectonic Significance: Acta Geologica Sinica, v. 89, n. 2, p. 272–288 (in Chinese with English abstract).
Li, P. W., Gao, R., Guan, Y., and Li, Q. S., 2006, Palaeomagnetic constraints on the final closure time of Solonker-Linxi suture: Journal of Jilin University (Earth Science Edition), v. 36, p. 744–758 (in Chinese with English abstract).
Li, S., Wilde, S. A., Wang, T., Xiao, W. J., and Guo, Q. Q., 2016, Latest Early Permian granitic magmatism in southern Inner Mongolia: Gondwana Research, v. 29, n. 1, p. 168–180, https://doi.org/10.1016/j.gr.2014.11.006
Li, W. B., Zhong, R. C., Xu, C., Song, B., and Qu, W. J., 2012, U-Pb and Re-Os geochronology of the Bainaimiao Cu-Mo-Au deposit, on the northern margin of the North China Craton, Central Asia Orogenic Belt: Implications for ore genesis and geodynamic setting: Ore Geology Reviews, v. 48, p. 139–150, https://doi.org/10.1016/j.oregeorev.2012.03.001
Li, Y. L., Zhou, H. W., Brouwer, F. M., Wijbrans, J. R., Zhong, Z. Q., and Liu, H. F., 2011, Tectonic significance of the Xilin Gol Complex, Inner Mongolia, China: Petrological, geochemical and U-Pb zircon age constraints: Journal of Asian Earth Sciences, v. 42, n. 5, p. 1018–1029, https://doi.org/10.1016/j.jseaes.2010.09.009
Li, Z. X., Bogdanova, S. V., Collins, A. S., Davidson, A., De Waele, B., Ernst, R. E., Fitzsimons, I. C. W., Fuck, R. A., Gladkochub, D. P., Jacobs, J., Karlstrom, K. E., Lu, S., Natapov, L. M., Pease, V., Pisarevsky, S. A., Thrane, K., and Vernikovsky, V., 2008, Assembly, configuration, and break-up history of Rodinia: A synthesis: Precambrian Research, v. 160, n. 1–2, p. 179–210, https://doi.org/10.1016/j.precamres.2007.04.021
Lian, C. Q., Li, G. Z., Yu, Y., Yao, F. J., Wang, P. J., and Cui, S. Y., 2021, LA-ICP-MS zircon U-Pb age and whole-rock geochemistry of the Triassic intrusive rocks in the Solon Obo area: Inner Mongolia and its geological significance: Earth Science, v. 46, p. 87–100.
Liu, C. H., Zhao, G. C., Liu, F. L., and Shi, J. R., 2017b, Detrital zircon U-Pb and Hf isotopic and whole-rock geochemical study of the Bayan Obo Group, northern margin of the North China Craton: Implications for Rodinia reconstruction: Precambrian Research, v. 303, p. 372–391, https://doi.org/10.1016/j.precamres.2017.04.033
Liu, D. Y., Jian, P., Zhang, Q., Zhang, F. Q., Shi, R. Y., Shi, G. H., Zhang, F. Q., and Tao, H., 2003, SHRIMP Dating of Adakites in the Tulingkai Ophiolite, Inner Mongolia: Evidence for the Early Paleozoic Subduction: Acta Geologica Sinica, v. 77, p. 317–330 (in Chinese with English abstract).
Liu, J. F., Chi, X. G., Zhang, X. Z., Ma, Z. H., Zhao, Z., Wang, T. F., Hu, Z. C., and Zhao, X. Y., 2009, Geochemical characteristic of Carboniferous quartz-diorite in the Southern Xiwuqi Area, Inner Mongolia and its tectonic significance: Acta Geologica Sinica, v. 83, p. 365–376 (in Chinese with English abstract).
Liu, Q., Zhao, G. C., Han, Y. G., Eizenhöfer, P. R., Zhu, Y. L., Hou, W. Z., and Zhang, X. R., 2017c, Timing of the final closure of the Paleo-Asian Ocean in the Alxa Terrane: Constraints from geochronology and geochemistry of Late Carboniferous to Permian gabbros and diorites: Lithos, v. 274–275, p. 19–30, https://doi.org/10.1016/j.lithos.2016.12.029
Liu, Q., Zhao, G. C., Han, Y. G., Eizenhöfer, P. R., Zhu, Y. L., Hou, W. Z., and Zhang, X. R. W. B., 2017d, Geochronology and geochemistry of Permian to Early Triassic granitoids in the Alxa Terrane: Constraints on the final closure of the Paleo-Asian Ocean: Lithosphere, v. 9, n. 4, p. 665–680, https://doi.org/10.1130/L646.1
Liu, Y. F., Nie, F. J., Jiang, S. H., Hou, W. R., Liang, Q. L., Zhang, K., and Liu, Y., 2012, Geochronology of Zhunsujihua molybdenum deposit in Sonid Left Banner: Inner Mongolia, and its geological significance: Mineral Deposits, v. 31, n. 1, p. 119–128. https://doi.org/10.3969/j.issn.0258-7106.2012.01.010
Liu, Y., Li, W., Feng, Z., Wen, Q., Neubauer, F., and Liang, C., 2017a, A review of the Paleozoic tectonics in the eastern part of Central Asian Orogenic Belt: Gondwana Research, v. 43, p. 123–148, https://doi.org/10.1016/j.gr.2016.03.013
Liu, Y. S., Gao, S., Hu, Z. C., Gao, C. G., Zong, K. Q., and Wang, D. B., 2010, Continental and oceanic crust recycling-induced melt-peridotite interactions in the Trans-North China Orogen: U-Pb dating, Hf isotopes and trace elements in zircons from mantle xenoliths: Journal of Petrology, v. 51, n. 1–2, p. 537–571, https://doi.org/10.1093/petrology/egp082
Lu, Y. H., and Li, W. B. L. Y., 2009, Time and tectonic setting of hosting porphyry of the Hadamiao gold deposit in Xianghuangqi, Inner Mongolia: Acta Petrologica Sinica, v. 25, p. 2615–2620, (in Chinese with English abstract).
Lu, Y. M., Pan, M., Qing, M., Zhang, Y. J., Han, X. J., and Chao, Y. Y., 2012, Zircon U-Pb age of gold-bearing granitic intrusive rocks in Bilihe gold deposit of Inner Mongolia and its geological significance: Acta Petrologica Sinica, v. 3, p. 993–1004 (in Chinese with English abstract).
Ludwig, K. R., 2001, Squid 102: A user's manual: Berkeley, California, Berkeley Geochronology Centre, Special Publication, p. 1–19.
User's manual for isoplot Ludwig, K. R., 3.00(2003)., a geochronological toolkit for microsoft excel: Berkeley, California, Berkeley Geochronology Center, p. 1–70.
Luo, H. L., Wu, T. R., Zhao, L., and He, Y. K. J. X., 2013, Geochemical Characteristics of Bayinzhurihe Pluton and Its Tectonic Significance, Bayan Obo, Inner Mongolia: Geological Journal of China Universities, v. 19, p. 123–132, (in Chinese with English abstract).
Miao, L. C., Liu, D. Y., Zhang, F. Q., Fan, W. M., Shi, Y. R., and Xie, H. Q., 2007, Zircon SHRIMP U–Pb ages of the “Xinghuadukou Group” in Hanjiayuanzi and Xinlin areas and the “Zhalantun Group” in Inner

Mongolia: Chinese Science Bulletin, v. 52, n. 8, p. 1112–1124, https://doi.org/10.1007/s11434-007-0131-2

Miao, L. C., Fan, W. M., Liu, D. Y., Zhang, F. Q., Shi, Y. R., and Guo, F., 2008, Geochronology and geochemistry of the Hegenshan ophiolitic complex: Implications for late-stage tectonic evolution of the Inner Mongolia-Daxinganling Orogenic Belt: Journal of Asian Earth Sciences, v. 32, n. 5–6, p. 348–370, https://doi.org/10.1016/j.jseaes.2007.11.005

Nasdala, L., Hofmeister, W., Norberg, N., Martinson, J. M., Corfu, F., Dörr, W., Kamo, S. L., Kennedy, A. K., Kronz, A., Reiners, P. W., Frei, D., Kosler, J., Wan, Y. S., Götze, J., Häger, T., Kröner, A., and Valley, J. W., 2008, Zircon M257: A homogeneous natural reference material for the ion microprobe U-Pb analysis of zircon: Geostandards and Geoanalytical Research, v. 32, n. 3, p. 247–265, https://doi.org/10.1111/j.1751-908X.2008.00914.x

Peng, P., Bleeker, W., Ernst, R. E., Söderlund, U., and McNicoll, V., 2011, U-Pb baddeleyite ages, distribution and geochemistry of 925 Ma mafic dykes and 900 Ma sills in the North China Craton: evidence for a Neoproterozoic mantle plume: Lithos: v. 127, n. 1–2, p. 210–221, https://doi.org/10.1016/j.lithos.2011.08.018

Piper, J. D. A., Jiasheng, Z., Huang, B., and Roberts, A. P., 2011, Palaeomagnetism of Precambrian dyke swarms in the North China Shield: The ~1.8 Ga LIP event and crustal consolidation in late Palaeoproterozoic times: Journal of Asian Earth Sciences, v. 41, n. 6, p. 504–524, https://doi.org/10.1016/j.jseaes.2011.03.010

Pirajno, F., Seltmann, R., and Yang, Y., 2011, A review of mineral systems and associated tectonic settings of northern Xinjiang, NW China: Geoscience Frontiers, v. 2, n. 2, p. 157–185, https://doi.org/10.1016/j.gsf.2011.03.006

Rojas-Agramonte, Y., Kröner, A., Demoux, A., Xia, X., Wang, W., Donskaya, T., Liu, D., and Sun, M., 2011, Detrital and xenocrystic zircon ages from Neoproterozoic to Palaeozoic arc terranes of Mongolia: Significance for the origin of crustal fragments in the Central Asian Orogenic Belt: Gondwana Research, v. 19, n. 3, p. 751–763, https://doi.org/10.1016/j.gr.2010.10.004

Sengör, A. M. C., and Natal'in, B. A., 1996, Turkic-type orogeny and its role in the making of the continental crust: Annual Review of Earth and Planetary Sciences, v. 24, p. 263–337, https://doi.org/10.1146/annurev.earth.24.1.263

Şengör, A. M. C., Natal'in, B. A., and Burtman, V. S., 1993, Evolution of the Altaid tectonic collage and Paleozoic crustal growth in Eurasia: Nature, v. 364, p. 299–307, https://doi.org/10.1038/364299a0

Shang, Q. H., 2004, Occurrences of Permian radiolarians in central and eastern Nei Mongol (Inner Mongolia) and their geological significance to the Northern China Orogen: Chinese Science Bulletin, v. 49, n. 24, p. 2613–2619, https://doi.org/10.1360/04wd0069

Shao, J. A., 1991, Crustal evolution in the middle part of the northern margin of the Sino-Korean Plate: Beijing, China, Peking University Publishing House, p. 1–135 (in Chinese with English abstract).

Shao, J. A., Tang, K. D., and He, G. Q., 2014, Early Permian tectono-palaeogeographic reconstruction of Inner Mongolia, China: Acta Petrologica Sinica, v. 30, p. 1858–1866 (in Chinese with English abstract).

Shen, S. Z., Zhang, H., Shang, Q. H., and Li, W. Z., 2006, Permian stratigraphy and correlation of Northeast China: A review: Journal of Asian Earth Sciences, v. 26, n. 3–4, p. 304–326, https://doi.org/10.1016/j.jseaes.2005.07.007

Shi, Y. R., Liu, D. Y., Zhang, Q., Jian, P., Zhang, F. Q., Miao, L. C., Shi, G. H., Zhang, L. Q., and Tao, H., 2004, SHRIMP geochronology of diorite granitoids in the Sonid Left banner area, Inner Mongolia: Acta Geologica Sinica, v. 78, n. 6, p. 789–799 (in Chinese with English abstract).

Shi, Y. R., Liu, D. Y., Zhang, Q., Jian, P., Zhang, F. Q., Miao, L. C., and Zhang, L. Q., 2007, SHRIMP U-Pb zircon dating of Triassic A-type granites in Sonid Zuoqi, central Inner Mongolia, China, and its tectonic implications: Geological Bulletin of China, v. 2, p. 183–189 (in Chinese with English abstract).

Shi, Y. R., Jian, P., Kröner, A., Li, L. L., Liu, C., and Zhang, W., 2016, Zircon ages and Hf isotopic compositions of Ordovician and Carboniferous granitoids from central Inner Mongolia and their significance for early and late Paleozoic evolution of the Central Asian Orogenic Belt: Journal of Asian Earth Sciences, v. 117, p. 153–169, https://doi.org/10.1016/j.jseaes.2015.12.007

Shi, Y. R., Zhang, W., Kröner, A., Li, L. L., and Jian, P., 2018, Cambrian ophiolite complexes in the Beishan area, China, southern margin of the Central Asian Orogenic Belt: Journal of Asian Earth Sciences, v. 153, p. 193–205, https://doi.org/10.1016/j.jseaes.2017.05.021

Sircombe, K. N., and Freeman, M. J., 1999, Provenance of detrital zircons on the Western Australia coastline–Implications for the geologic history of the Perth basin and denudation of the Yilgarn craton: Geology, v. 27, n. 10, p. 879–882, https://doi.org/10.1130/0091-7613(1999)027<0879:PODZOT>2.3.CO;2

Song, D., Xiao, W., Windley, B. F., Han, C., and Tian, Z., 2015, A Paleozoic Japan-type subduction-accretion system in the Beishan orogenic collage, southern Central Asian Orogenic Belt: Lithos, v. 224–225, p. 195–213, https://doi.org/10.1016/j.lithos.2015.03.005

Sun, D. Y., Wu, F. Y., Zhang, Y. B., and Gao, S. (2004).The final closing time of the west Lamulun River–Changchun-Yanji plate suture zone: Evidence from the Dayushan granitic pluton, Jilin Province: Journal of Jilin University (Earth Science Edition), v. 34, p. 174–181 (in Chinese with English abstract).

Sun, L. X., Ren, B. F., Zhao, F. Q., Gu, Y. C., Li, Y. F., and Liu, H., 2013, Zircon U–Pb dating and Hf isotopic compositions of the Mesoproterozoic granitic gneiss in Xilinhot Block, Inner Mongolia: Geological Bulletin China, v. 32, p. 327–340 (in Chinese with English abstract).

Tang, J., He, D., Li, D., and Ma, D., 2015, Large-scale thrusting at the northern Junggar Basin since Cretaceous and its implications for the rejuvenation of the Central Asian Orogenic Belt: Geoscience Frontiers, v. 6, n. 2, p. 227–246, https://doi.org/10.1016/j.gsf.2014.07.003

Tang, K. D., 1990, Tectonic development of Paleozoic fold belts at the northern margin of the Sino-Korean Craton: Tectonics, v. 9, n. 2, p. 249–260, https://doi.org/10.1029/TC009i002p00249
Tang, K. D., Shao, J. A., and Li, Y. F., 2011, SongnenMassif and its research significance: Earth Science Frontiers, v. 18, n. 3, p. 57–65 (in Chinese with English abstract).
Tong, Y., Hong, D. W., Wang, T., Shi, X. J., Zhang, J. J., and Zeng, T., 2010, Spatial and temporal distribution of granitoids in the middle segment of the Sino-Mongolian border and its tectonic and metallogenic implications: Acta Geoscientica Sinica, v. 31, n. 3, p. 395–412, (in Chinese with English abstract).
Wang, B., Faure, M., Shu, L., de Jong, K., Charvet, J., Cluzel, D., Jahn, B.-M., Chen, Y., and Ruffet, G., 2010, Structural and geochronological study of high-pressure metamorphic rocks in the Kekesu Section (northwestern China): Implications for the Late Paleozoic tectonics of the southern Tianshan: The Journal of Geology, v. 118, n. 1, p. 59–77, https://doi.org/10.1086/648531
Wang, C., Liu, L., Che, Z., He, S., Li, R., Yang, W., Cao, Y., and Zhu, X., 2009, Zircon U–Pb and Hf isotopic from the east segment of Tiekelike tectonic belt: constraints on the timing of Precambrian basement at the southwestern margin of Tarim China: Acta Geologica Sinica, v. 83, p. 1647–1656.
Wang, H. R., Zhao, H. G., Qiao, J. X., and Gao, S. H., 2013, Theory and application of zircon U-Pb isopote dating technique: Geology and Resources, v. 3, p. 229–232 (in Chinese with English abstract).
Wang, J., Sun, F. Y., Li, B. L., Wang, Y. D., and Li, R. H., 2016, Age, etrogenesis and Tectonic Implications of Permian Hornblendite in Tugurige, rad Zhongqi, Inner Mongolia: Earth Science, v. 41, n. 5, p. 792–808 (in Chinese with English abstract).
Wang, Q., Liu, X. Y., and Li, J. Y., 1991, Paleoplate tectonics in Nei Mongol of China: Bulletin of the Chinese Academy of Geological Sciences, v. 22, p. 1–19 (in Chinese with English abstract).
Wilde, S. A., Wu, F. Y., and Zhao, G. C., 2010, The Khanka Block: NE China, and its significance to the evolution of the Central Asian Orogenic Belt and continental accretion: Geological Society, London, Special Publications, v. 338, p. 117–137, https://doi.org/10.1144/SP338.6
Williams, I. S., 1997, U-Th-Pb geochronology by ion microprobe, *in* McKibben, M. A., Shanks, W. C. III., and Ridley, W. L., editors, Applications of Microanalytical Techniques to Understanding Mineralizing Processes: Reviews in Economic Geology, v. 7, p. 1–35, https://doi.org/10.5382/Rev.07.01
Windley, B. F., Alexeiev, D., Xiao, W., Kröner, A., and Badarch, G., 2007, Tectonic models for accretion of the Central Asian Orogenic Belt: Journal of the Geological Society, v. 164, n. 1, p. 31–47, https://doi.org/10.1144/0016-76492006-022
Wu, F. Y., Li, X. H., Zheng, Y. F., and Gao, S., 2007a, Lu-Hf isotopic systematics and their applications in petrology: Acta Petrologica Sinica, v. 23, p. 185–220 (in Chinese with English abstract).
Wu, F. Y., Yang, J. H., Wilde, S. A., Liu, X. M., Guo, J. H., and Zhai, M. G., 2007b, Detrital zircon U-Pb and Hf isotopic constraints on the crustal evolution of North Korea: Precambrian Research: Precambrian Research, v. 159, n. 3–4, p. 155–177, https://doi.org/10.1016/j.precamres.2007.06.007
Wu, X. C., Shi, Y. R., and Anderson, J. L., 2020, Provenance analysis of Permian sandstones from the Solonker area in central Inner Mongolia: Geological Journal, v. 55, n. 3, p. 2110–2128, https://doi.org/10.1002/gj.3715
Xiao, W. J., Windley, B. F., Hao, J., and Zhai, M. G., 2003, Accretion leading to collision and the Permian Solonker suture, Inner Mongolia, China: Termination of the Central Asian Orogenic Belt: Tectonics, v. 22, n. 6, p. 1069–1090, https://doi.org/10.1029/2002TC001484
Xiao, W. J., Kröner, A., and Windley, B., 2009, Geodynamic evolution of Central Asia in the Paleozoic and Mesozoic: International Journal of Earth Sciences, v. 98, p. 1185–1188, https://doi.org/10.1007/s00531-009-0418-4
Xiao, W. J., Windley, B. F., Allen, M. B., and Han, C., 2013, Paleozoic multiple accretionary and collisional tectonics of the Chinese Tianshan orogenic collage: Gondwana Research, v. 23, n. 4, p. 1316–1341, https://doi.org/10.1016/j.gr.2012.01.012
Xiao, W. J., Windley, B. F., Sun, S., Li, J. L., Huang, B. C., Han, C. M., Yuan, C., Sun, M., and Chen, H. L., 2015, A tale of amalgamation of three Permo-Triassic Collage Systems in Central Asia: Oroclines, sutures, and terminal accretion: Annual Review of Earth and Planetary Sciences, v. 43, p. 477–507, https://doi.org/10.1146/annurev-earth-060614-105254
Xiao, W. J., Windley, B. F., Han, C. M., Liu, W., Wan, B., Zhang, J. E., Ao, S. J., Zhang, Z. Y., and Song, D. F., 2018, Late Paleozoic to early Triassic multiple roll-back and oroclinal bending of the Mongolia collage in Central Asia: Earth-Science Reviews, v. 186, p. 94–128, https://doi.org/10.1016/j.earscirev.2017.09.020
Xin, W., Wang, L., and Wang, Y. D., 2016, Zircon U-Pb geochronology and geochemistry of Zhungashun granodiorites in Urad Zhongqi: Inner Mongolia: Global Geology, v. 35, n. 4, p. 931–941 (in Chinese with English abstract).
Xu, B., and Chen, B., 1997, Framework and evolution of the middle Paleozoic orogenic belt between Siberian and North China plates in northern Inner Mongolia: Science in China Series D: Earth Sciences, v. 40, p. 463–469 (in Chinese with English abstract), https://doi.org/10.1007/BF02877610
Xu, B., Charvet, J., Chen, Y., Zhao, P., and Shi, G. Z., 2013, Middle Paleozoic convergent orogenic belts in western Inner Mongolia (China): Framework, kinematics, geochronology and implications for tectonic evolution of the Central Asian Orogenic Belt: Gondwana Research, v. 23, n. 4, p. 1342–1364, https://doi.org/10.1016/j.gr.2012.05.015
Xu, L. Q., Ju, W. X., Liu, C., He, H. Y., and Li, M. Y., 2012, Sr-Yb classification and genesis of Late Carboniferous granites in Arenshaobu area of Erenhot, Inner Mongolia: Geological Bulletin of China, v. 31, n. 9, p. 1410–1419 (in Chinese with English abstract).
Xue, J. P., Liu, M. Y., Li, G. Z., Zhao, G. M., Wu, C. J., Li, C. Y., Liu, Y. X., Liang, Y. S., and Lian, C. Q., 2018, Zircon geochronology and geochemistry of Haer Bogetuoer TTG rock, Solonker zone, Inner

Mongolia and their tectonic implications: Earth Science Frontiers, v. 25, p. 230–239 (in Chinese with English abstract).
Yang, S. H., Miao, L. C., Zhang, F. C., Meng, Q. R., Zhu, M. S., Baatar, M., and Anaad, C., 2016, Zircon age and geochemistry of the Tost bimodal volcanic rocks: Constraints on the Early Carboniferous tectonic evolution of the South Mongolia: Journal of Asian Earth Sciences, v. 120, p. 29–42, https://doi.org/10.1016/j.jseaes.2016.01.021
Zhai, M. G., Guo, J. H., and Liu, W. J., 2005, Neoarchean to Paleoproterozoic continental evolution and tectonic history of the North China Craton: A review: Journal of Asian Earth Sciences, v. 24, n. 5, p. 547–561, https://doi.org/10.1016/j.jseaes.2004.01.018
Zhang, S. H., Zhao, Y., Song, B., Hu, J. M., Liu, S. W., Yang, Y. H., Chen, F. K., Liu, X. M., and Liu, J., 2009, Contrasting Late Carboniferous and Late Permian-Middle Triassic intrusive suites from the northern margin of the North China craton: Geochronology, petrogenesis and tectonic implications: Geological Society of America Bulletin, v. 121, n. 1–2, p. 181–200, https://doi.org/10.1130/B26157.1
Zhang, S. H., Zhao, Y., Ye, H., Liu, J. M., and Hu, Z. C., 2014c, Origin and evolution of the Bainaimiao arc belt: Implications for crustal growth in the southern Central Asian orogenic belt: GSA Bulletin, v. 126, n. 9–10, p. 1275–1300, https://doi.org/10.1130/B31042.1
Zhang, W., Jian, P., Kröner, A., and Shi, Y. R., 2013, Magmatic and metamorphic development of an early to mid-Paleozoic continental margin arc in the southernmost Central Asian Orogenic Belt, Inner Mongolia: Journal of Asian Earth Sciences, v. 72, p. 63–74, https://doi.org/10.1016/j.jseaes.2012.05.025
Zhang, X. H., Zhang, H. F., Tang, Y. J., Wilde, S. A., and Hu, Z. C., 2008, Geochemistry of Permian bimodal volcanic rocks from central Inner Mongolia, North China: Implication for tectonic setting and Phanerozoic continental growth in Central Asian Orogenic Belt: Chemical Geology: Chemical Geology, v. 249, n. 3–4, p. 262–281, https://doi.org/10.1016/j.chemgeo.2008.01.005
Zhang, X. R., Zhao, G. C., öfer, P. R., Sun, M., Han, Y. G., Hou, W. Z., Liu, D. X., Wang, B., Liu, Q., Xu, B., and Zhu, C. Y., 2016, Tectonic transition from Late Carboniferous subduction to Early Permian post-collisional extension in the Eastern Tianshan, NW China: Insights from geochronology and geochemistry of mafic–intermediate intrusions: Lithos, v. 256–257, p. 269–281, https://doi.org/10.1016/j.lithos.2016.04.006
Zhang, Y. S., Tian, S. G., Li, Z. S., Gong, Y. X., Xing, E. Y., Wang, Z. Z., Zhai, D. X., Jie, C., Kui, S., and Meng, W., 2014a, Discovery of marine fossils in the upper part of the Permian Linxi Formation in Lopingian: Chinese Science Bulletin, v. 59, n. 1, p. 62–74, https://doi.org/10.1007/s11434-013-0036-1
Zhang, Z., Zhang, H. F., Shao, J. A., Ying, J. F., Yang, Y. H., and Santosh, M., 2014b, Mantle upwelling during Permian to Triassic in the northern margin of the North China Craton: Constraints from southern Inner Mongolia: Journal of Asian Earth Sciences, v. 79, Part A, p. 112–129, https://doi.org/10.1016/j.jseaes.2013.09.015
Zhao, G. C., Cawood, P. A., Wilde, S. A., and Sun, M., 2002, Review of global 2.1–1.8 Ga orogens: Implications for a pre-Rodinia supercontinent: Earth-Science Reviews: Earth-Science Reviews, v. 59, n. 1–4, p. 125–162, https://doi.org/10.1016/S0012-8252(02)00073-9
Zhao, G., Sun, M., Wilde, S. A., and Sanzhong, L., 2005, Late Archean to Paleoproterozoic evolution of the North China Craton: Key issues revisited: Precambrian Research, v. 136, n. 2, p. 177–202, https://doi.org/10.1016/j.precamres.2004.10.002
Zhao, G. C., Wang, Y. J., Huang, B. C., Dong, Y. P., Li, S. Z., Zhang, G. W., and Yu, S., 2018, Geological reconstructions of the East Asian blocks: From the breakup of Rodinia to the assembly of Pangea: Earth-Science Reviews, v. 186, p. 262–286, https://doi.org/10.1016/j.earscirev.2018.10.003
Zhao, L., Wu, T. R., and Luo, H. L., 2011, SHRIMP U-Pb dating, geochemistry and tectonic implications of the Beiqigetao gabbros in Urad Zhongqi area, Inner Mongolia: Acta Petrologica Sinica, v. 10, p. 3071–3082 (in Chinese with English abstract).
Zhao, Y. L., Li, W. M., Wen, Q. B., Liang, C. Y., Feng, Z. Q., Zhou, J. P., and Shen, L., 2016, Late Paleozoic tectonic framework of eastern Inner Mongolia: Evidence from the detrital zircon U-Pb ages of the Mid-late Permian to Early Triassic sandstones: Acta Petrologica Sinica, v. 32, n. 9, p. 2807–2822 (in Chinese with English Abstract).
Zhou, J. B., Wilde, S. A., Zhang, X. Z., Liu, F. L., and Liu, J. H., 2012, Detrital zircons from Phanerozoic rocks of the Songliao Block, NE China: Evidence and tectonic implications: Journal of Asian Earth Sciences, v. 47, p. 21–34, https://doi.org/10.1016/j.jseaes.2011.05.004
Zhou, J. B., Wilde, S. A., Zhao, G. C., and Han, J., 2018, Nature and assembly of microcontinental blocks within the Paleo-Asian Ocean: Earth-Science Reviews, v. 186, p. 76–93, https://doi.org/10.1016/j.earscirev.2017.01.012
Zhu, M. S., Miao, L. C., Baatar, M., Zhang, F. C., Anaad, C., Yang, S. H., and Li, X. B., 2016a, Early Paleozoic oceanic inliers and reconstruction of accretionary tectonics in the Middle Gobi region, Mongolia: Evidence from SHRIMP zircon U-Pb dating and geochemistry: Journal of Asian Earth Sciences, v. 127, p. 300–313, https://doi.org/10.1016/j.jseaes.2016.06.018
——— 2016b, Late Paleozoic magmatic record of Middle Gobi area, South Mongolia and its implications for tectonic evolution: Evidences from zircon U-Pb dating and geochemistry: Journal of Asian Earth Sciences, v. 115, p. 507–519, https://doi.org/10.1016/j.jseaes.2015.11.002